Showmik Dasgupta

Modelling and testing of hybrid channeling plates for thermal management of batteries for electrical vehicles

Thesis submitted for the degree of Masters of Science in Technology

Aalto University, School of Engineering
Espoo, Finland. December 2017.
Supervisor: Professor Pedro Vilaça
Advisor: Heikki Karvinen

Author Showmik Dasgupta

Title of thesis Modelling and testing of hybrid channeling plates for thermal management of batteries for electrical vehicles

Master programme Mechanical Engineering **Code** IA3027

Thesis supervisor Professor Pedro Vilaça

Thesis advisor(s) Heikki Karvinen

Date 12.12.2017 **Number of pages** 47+1 **Language** English

Abstract

In this work, Base Cooling Plates (BCP) used in thermal management of batteries for Electric Vehicle (EV) are designed taking advantage of the new advanced production technique: The Hybrid Friction Stir Channeling (HFSC). The HFSC is a new friction stir based solution for producing internal, closed channels created simultaneously during welding of multiple metal plates. The channels are produced in a single step, with any path and constant or continuously modified shape along the path. In this work, the HFSC was applied to produce BCP made of a skin of copper with aluminum-channeled ribs. The performance of the HFSC to produce BCP was compared with other channeling methods, such as, milling and conventional Friction Stir Channeling (FSC), applied to monolithic aluminum plates.

Commercial Computational Fluid Dynamics (CFD) software: Fluent, was used as the main tool to design and optimize the conformal cooling strategy, for each one of the channeling methods. The CFD model was applied in the design of the Base Cooling Plates with simulation of the heat and fluid flow. The CFD simulation model was validated using experimental procedures, mainly regarding the influence of the different surface finishing of the channels, in the heat transference models into the wall. Upon validation, the CFD model was used to minimize the cost and time associated with alternative optimization strategies based on experimental testing of different concepts. The performance parameters used as criteria in the development of the best conformal cooling solution was the cost, weight and thermal efficiency, by minimizing the peak temperature and temperature amplitude in the BCP. The HFSC enables to use a thin sheet of copper with superior thermal capabilities as a base plate of the BCP. Using copper along with HFSC, enables higher corrosion resistance, and retaining the mechanical resistance until much higher temperatures, when compared with utilization of monolithic aluminum plate. The thin copper with the stiffness given by the aluminum channeled ribs, opens up the possibility to use lesser amount of material, lowering the weight and cost of the final assembled system.

The stationary state results confirmed that the peak temperature in the BCP made with conventional FSC is better than made with milling in about 4 Kelvin. Considering that, the channels have exactly the same path and size, this improvement is resulting from the different surface finishing. The HFSC process provided the superior thermal properties of all the models, while using less amount of materials. Compared with the solution of channels produced by FSC, the peak temperature of the best HFSC cooling plate was about 7 % (or 18 Kelvin) lower. The structural weight and water volume within the HFSC cooling plate was lower in 10% and 11.5%, respectively.

Keywords Keywords Hybrid Friction Stir Channeling, Channeling, Welding, Conformal cooling, Battery cooling plates, Copper, Aluminium Alloy, Electrical Vehicles, Batteries, Ansys, CFD, k-epsilon model, Roughness

Acknowledgement

I would like to take this opportunity to thank my supervisor Professor Pedro Vilaca for his continuous support throughout this process. I am grateful for being given the chance to work with the Hybrid channeling process, where I gained a lot of useful knowledge. Over the course of the thesis, his words of encouragement provided me with the strength to keep going when things were not working out the way it should be. His passion for his work is astounding and his drive for innovations and inventions inspired me greatly.

I would also like to thank my supervisor, Heikki Karvinen for his help and support whenever I needed it. I would have been overwhelmed with all the work had he not given me hands on instruction on how to operate the machines in the lab and helped me prepare samples.

I would also like to thank my colleagues for their company while I worked here.

I would also like to thank my family for their words of advice, support and encouragement when the work got tedious. Their love and affection has heled me through the rough times.

Showmik Das Gupta

Showmik Dasgupta

Contents

Symbols and Abbreviations

EV	Electric Vehicle
BCP	Base Cooling Plate
HFSC	Hybrid Friction Stir Channeling
CFD	Computational Fluid Dynamics
Li-ion	Lithium-ion
IC	Internal Combustion
PHEV	Plug In Hybrid Vehicle
FSC	Friction Stir Channeling
CAD	Computer Aided Designing
FSW	Friction Stir Welding
TTS	Tool Travel Speed
TRS	Tool Rotation Speed

Table of Figures

1 Introduction

1.1 Scope of the thesis

This thesis aims at comparing between channels made in Base Cooling Plate (BCP) for Electrical Vehicle (EV) batteries by using Milling, Friction Stir Channeling (FSC) and Hybrid Friction Stir Channeling (HFSC) processes. The comparing criteria selected are maximum and minimum temperature of the BCP, temperature gradient across the BCP, material cost and weight of the assembly. It also aims to come up with a conformal cooling channel path using the HFSC process to provide better cooling options for BCP while also lowering the material cost and weight. Computational Fluid Dynamics (CFD) simulation software Asnys-Fluent is used to carry out the comparison process.

Electric vehicles are becoming more and more popular as the fear for global energy crisis looms over the head. Even traditional internal combustion (IC) engine car manufacturers like BMW, General Motors, Toyota etc. have been getting into the EV market. BMW with its i3, General Motors with Chevrolet Bolt, Toyota with its Plug in Hybrid Electric Vehicle (PHEV) Prius have taken the vehicle industry by storm. New companies such as Tesla, which predominantly produces EVs, has made its mark on the industry in a very short span of time. Currently, EVs are quite expensive to purchase compared to basic IC engine cars, but their operational and lifetime costs are significantly lower. One sector where the base EVs lag behind traditional gasoline fueled vehicles is their range. Gasoline fueled cars can travel much further on a full tank than their EV counterpart can do within one charge-discharge cycle. Therefore, a lot of research has been carried out on how to get the highest possible range out of the EV batteries. The EV batteries currently used by majority of the EV manufacturers are lithium-ion (Li-ion) batteries whether in cylindrical form (Panasonic) or in prismatic form (LG, Samsung SDI). One factor that heavily influences the range output from Li-ion EV batteries is the operating temperature. When the batteries operated out of their optimal temperature range, the output from these batteries goes down significantly. Thus, it is essential to keep the batteries working within the optimal temperature range so as to get the maximum output from them. The batteries generate a lot of heat during charging and discharging cycles due to internal resistance within the batteries. This heats up the batteries to a temperature out of their optimal range. To bring them down to their optimal working temperature, active or passive cooling solutions needs to be provided. The cooling solutions need to be leak-proof (so as not to damage the batteries or cause corrosion to other components), compact (be able to be installed inside a small car) and light (to reduce the overall weight of the car). Moreover, the temperature gradient across the plate needs to be at a minimum to provide uniform cooling for the battery surface. With all these factors in mind, different designs of the cooling path of BCP were simulated in order to find the best solution that maximizes cooling power and minimizes the temperature gradient and the weight of the system.

Among the three different types of the channeling process, only HFSC can provide the means to produce a channel with free-path while welding two materials (similar or dissimilar) at the same time. HFSC process creates a closed channel while also welding the multiple materials together. Therefore, for the HFSC process, there was the added benefit of being able to use a thin sheet of copper plate with superior thermal properties without significantly increasing the overall cost of the system. Moreover, since it was possible to produce conformal cooling channel and weld with HFSC, designs and simulations were performed to check if the copper helped with lowering the temperature gradient across the plate while using less amount of aluminum.

1.2 Work Plan and Objectives

This thesis focusses on the use of a commercial CFD simulation software to compare the differences in cooling capacity of the BCP cooling channels manufactured by traditional Milling, FSC and HFSC processes. For the HFSC process, conformal cooling channels were designed using thin sheet of copper as base plate, because of its superior thermal properties, and narrow ribs of aluminum as the source of heat extraction from the copper plate, which was then transferred to the liquid coolant.

This thesis relies heavily on the simulations since it is easier to test out multiple ideas and concepts thus reducing the necessity of making several up to scale BCP models and significantly reduces the costs and time spent on experimentation of different concepts.

The objectives of the thesis were:

- To analyze and study the current methods of creating BCPs, establishing the drawbacks of the current methods.
- To develop Computer Aided Design (CAD) models of different conformal cooling strategies for HFSC process along with models for the current BCP channeling strategy using milling methods and FSC methods.
- To develop a CFD model of the different design solutions and to simulate the heat transfer and fluid flow in steady state analysis were carried out on the models.
- To validate the model using experimental setup.
- To compare between the models of BCP made with Milling, FSC and HFSC.
    - o Find advantages or disadvantages of the BCPs made with the three methods.
    - o Determine the reason for the differences (if any).
- Choose the best possible method and perform cost and weight analysis.
- Further improve the model to check if there are any benefits.

1.3 Organization of the Thesis

This thesis consists of 9 (nine) chapters. The second chapter of the thesis is State of the Art, which comes after the Introduction. This chapter explores the current state of EV batteries and cooling techniques used for cooling them. Fundamentals of the HFSC processes is also included in this chapter.

Chapter 3 includes the theories and equations involved in simulating the heat and mass flow in the models. It includes the governing equations used by CFD softwares to simulate heat and mass flow.

Chapter 4 delves into the material properties of Copper and Aluminum in order to justify why they were chosen as the two materials for the implementation of the HFSC method.

Chapter 5 deals with the modelling of the simulation. This chapter explains all the boundary conditions, initial conditions, thermal loads and flow rates used while modelling the BCP simulation.

Chapter 6 details the experimental validation procedures that were carried out to validate the model.

Chapter 7 deals with comparing the simulation results of the BCPs made by milling, FSC and HFSC. This also includes the simulation results of the different iterations of HFSC conformal cooling models that was designed.

Chapter 8 is the penultimate chapter which deals with the selection of the best possible solution from the simulation results and performing structural, weight and cost analysis on it.

Chapter 9 is the last chapter of this thesis, which gives an overall summary of the work done in the thesis and also includes comment on what can be done in the future.

2 State of the Art

2.1 Friction Stir Channeling

Friction Stir Welding (FSW) was developed and patented in 1991 by Thomas et al.(1) at The Welding Institute in the U.K. as a solid state welding process. In this process, a non consumable tool is inserted and rotated along the plane of two materials to be joined. The materials are clamped and butted together to stop any movement. The tool is plunged until the shoulder touches the surface and then moved forward. As the tool traverses forward, the heat due to friction and mechanical churning of the materials causes the weld zone materials to soften without melting. As the heat goes down, the mixed materials forms the weld.

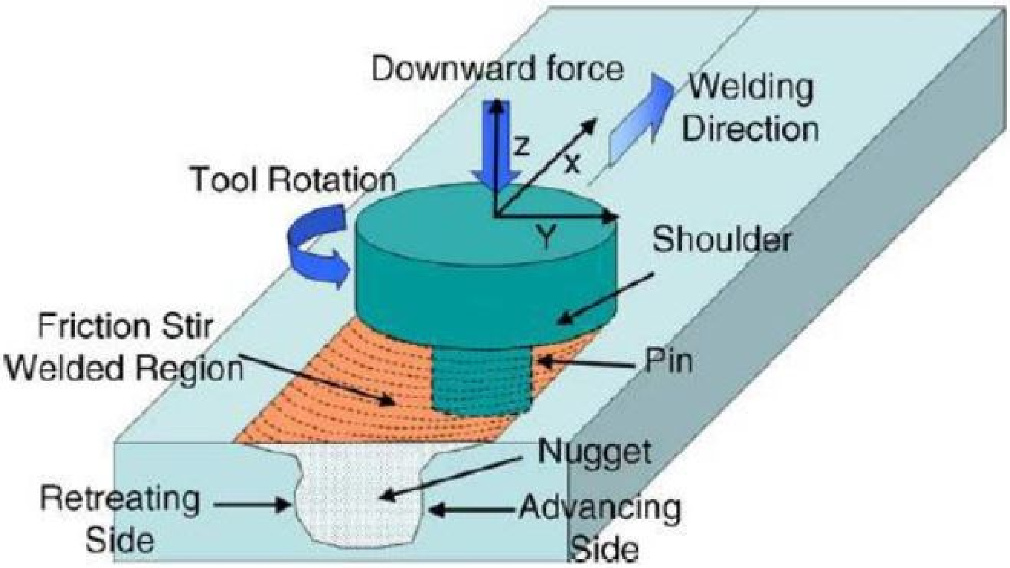

Figure 1 FSW process(2)

This process is considered widely used for joining processes because it allows for the materials to be welded with melting or reaching the fusion temperature. One of the biggest drawbacks of this process is that it sometimes caused wormhole in the interior.

In 2005 however, Mishra developed and patented the idea of using this defect to create a closed channel inside the workpiece (2, 3). He realized that if the processing parameters are not correct, the wormhole is almost always formed. He identified this processing parameter to be distance of the shoulder from the workpiece. Mishra showed that using this wormhole defect, a continuous closed channel can be created in the material (3). He commented that this process can be used in manufacturing small heat exchangers. This process he named as Friction Stir Channeling process. Later on, Mishra along with Balasubramanian (4) characterized the channels.

2.2 Hybrid Friction Stir Channeling (HFSC)

HFSC is a newly developed process of creating closed internal channel in a material while also joining it with other material(s). This process incorporates the fundamentals of FSC and FSW. In this technique, a threaded tool with a welding head is dipped into the base component while the specially designed tool tip penetrates the second component. As the tool is driven forwards, it produces a closed channel with the top of the channel also getting welded to the second component.

HFSC is a solid state welding and channeling process which produces channels with rough surfaces inside the components. These rough surfaces increases the chance of the flow inside the channel being turbulent, which in turn helps in providing better thermal capacities to the assembly.

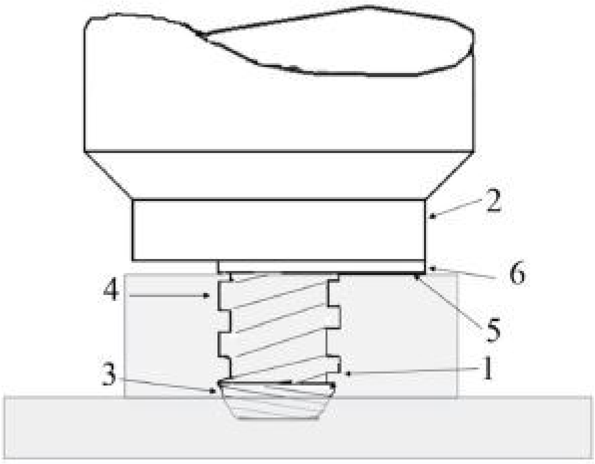

Figure 2 HFSC TOOL (5)

The figure shows a HFSC tool which is used in the channeling process. In this tool, the section 3 is the part that welds the two material together, while section 5 and 6 forms the ceiling of the channel by removing material in form of flashes. This tool can thus create the channel and the weld at one go. Since closed continuous channels can be formed without any limitation of shape, this gives rise to the chances of designing conformal cooling channels with the help of HFSC process.

Much work has been done in the field of developing HFSC tools and analyzing the parameters for ongoing repeatability. It was seen that the best results for the channeling process is observed at Tool Travel Speed (TTS) of 90 mm/min and a Tool Rotation Speed (TRS) of 300 rpm(5). The thesis work done by Daniel Nordal at Aalto also comes up with a new tool design for maximum repeatability and reliability while also producing less flash. Leak tests and

Microhardness measurements were also done in the thesis which showed improved stability of the channel.

Example of the channel made by the HFSC process is shown in the figure below.

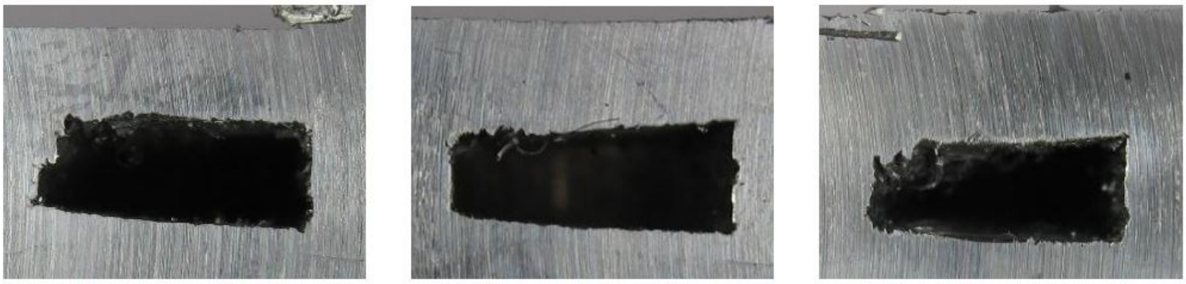

Figure 3 Channels made by HFSC techniques

2.3 Electric Vehicle Batteries

Electric vehicle (EV) has been in the market for a while, but only recently, with the looming energy crisis, they have gained a lot of popularity. EVs are essentially vehicles which run on electricity, rather than conventional gasoline fuels.

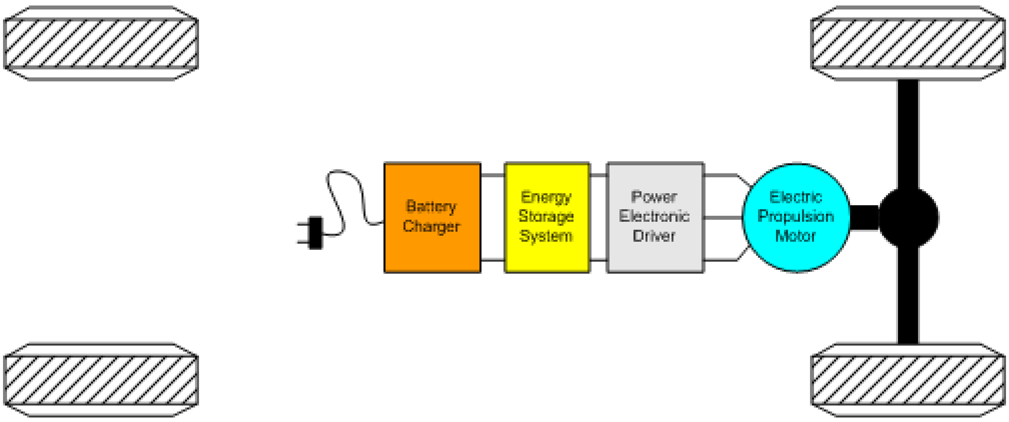

Figure 4 Schematic diagram of EV system(6)

Figure 4 shows the schematic diagram of an EV. In this, the Energy Storage System (ESS) is the battery which provides power to the motor for driving the car. In other words, Batteries are the equivalent of an IC engine in a regular car. Battery is in fact, the most important component of the EV system. Batteries determine the range of the vehicle, which is one of the most important selling point of the cars. Battery packs come in the range of 10-100 kWh which can provide a range anywhere between 60 to 200 miles. Cars like BMW i3 provides a range of 114 miles with a mere 33 kWh battery whereas high end cars like Tesla can provide a range of about 300 miles with a 100 kWh battery(7).

The batteries in the EV vehicle are mainly of 3 types:

- Cylindrical
- Prismatic
- Pouch

There is also a fourth type of cell called Button cell but they are not used in EVs. Of these types, Prismatic cells are most commonly used. Vehicle manufacturers like BMW and GM uses Prismatic cell type batteries predominantly whereas Tesla makes use of Cylindrical type batteries.

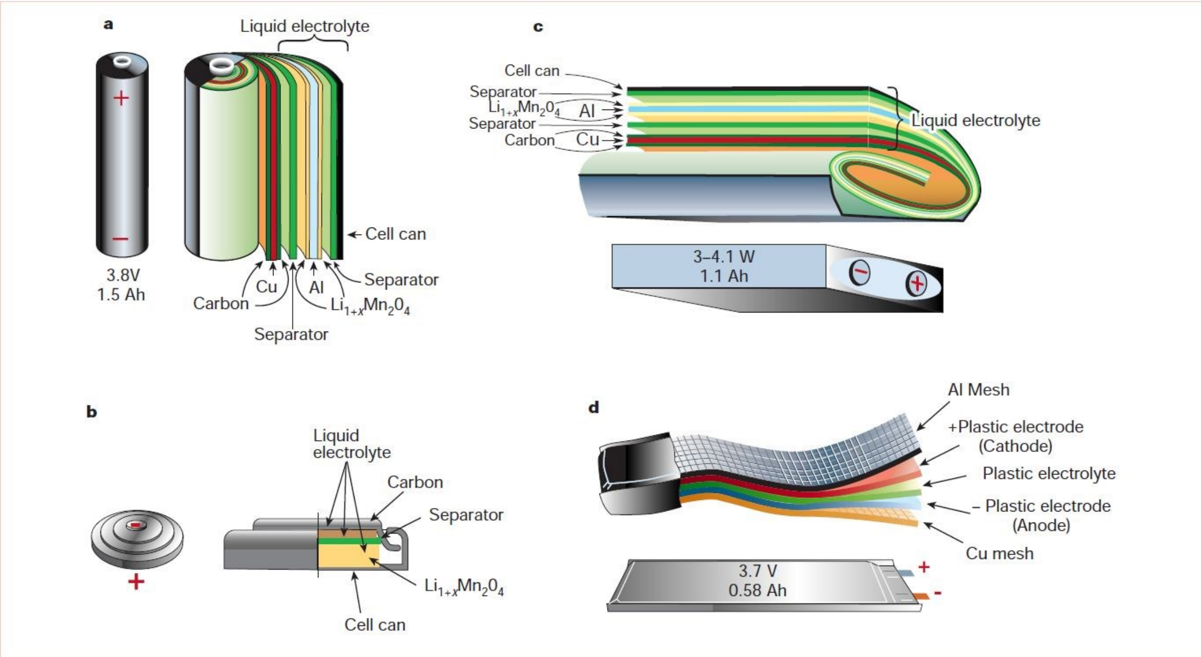

Figure 5 Battery types(8)

In Figure Figure 5, (a) is the cylindrical type battery whereas (c) shows the prismatic cell battery. A lot of progress has been made in battery technologies over the years and the car companies are collaborating with the battery manufacturing companies to advance the research.

Company	Country	Vehicle model	Battery technology
GM	USA	Chevy-Volt	Li-ion
		Saturn Vue Hybrid	NiMH
Ford	USA	Escape, Fusion, MKZ HEV	NiMH
		Escape PHEV	Li-ion
Toyota	Japan	Prius, Lexus	NiMH
Honda	Japan	Civic, Insight	NiMH
Hyundai	South Korea	Sonata	Lithium polymer
Chrysler	USA	Chrysler 200C EV	Li-ion
BMW	Germany	X6	NiMH
		Mini E (2012)	Li-ion
BYD	China	E6	Li-ion
Daimler Benz	Germany	ML450, S400	NiMH
		Smart EV (2010)	Li-ion
Mitsubishi	Japan	iMiEV (2010)	Li-ion
Nissan	Japan	Altima	NiMH
		Leaf EV (2010)	Li-ion
Tesla	USA	Roadster (2009)	Li-ion
Think	Norway	Think EV	Li-ion, Sodium/Metal Chloride

Figure 6 Car manufacturers and type of battery used(9)

Figure 6 shows another category by which the batteries can be differentiated. As can be seen, most car manufacturers use Li-ion batteries. They can provide good range at a reasonable price and have been the focus of major battery developers.

These batteries when charged and discharged releases energy in the form of heat. This heat is a direct result of the internal resistance of batteries. Although the heat generated is nowhere near the level of IC engines, the batteries still need to be cooled down. This is because the batteries operate at an optimal temperature range(10). Outside of this range, the batteries lose efficiency which results in lower battery life and mileage. So, Battery cooling is a very important part of the EV system.

Currently, several types of cooling exists. In this thesis, the battery cooling techniques of Prismatic cell and Cylindrical cell batteries are looked at.

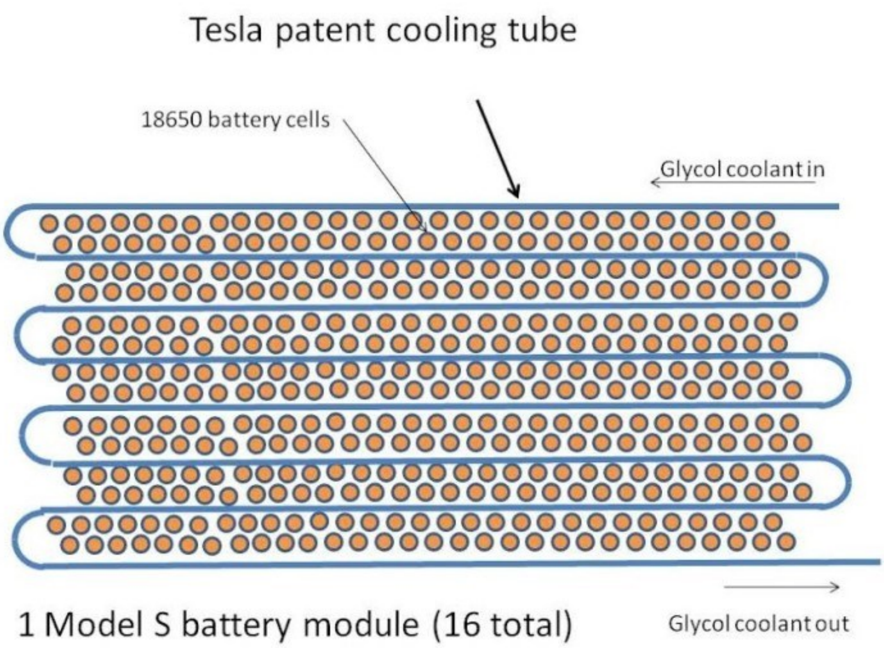

Figure 7 Tesla cooling technique(11)

Figure 7 shows the cooling system used by Tesla motors. In this system, a liquid coolant cools the cylindrical type batteries used by Tesla. This process is cheap but not reliable. By the time the coolant reaches the end, it is already heated up and cannot take up any further heat. Also, since it is in series, if there is a leak anywhere down the cooling channel, it results in failure of the system

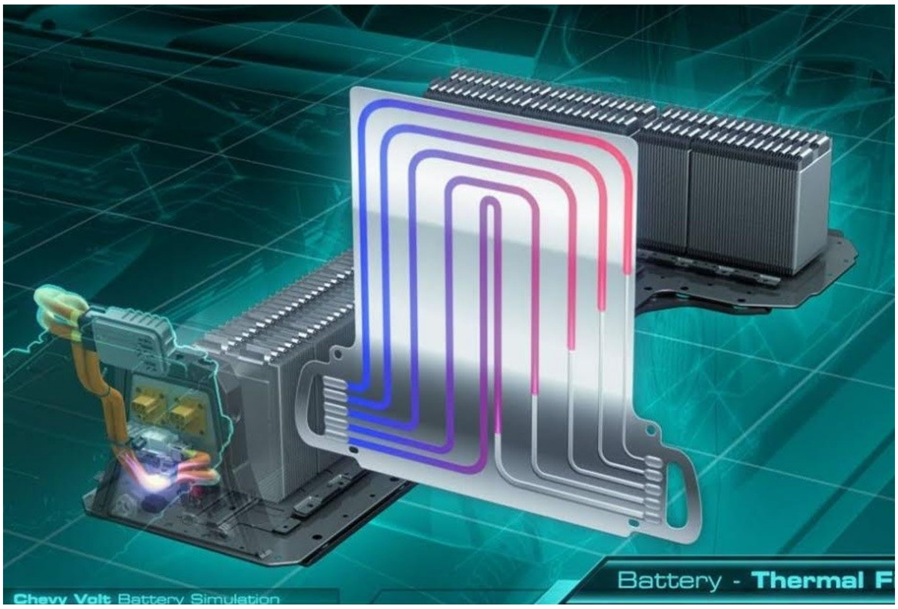

. Figure 8 GM Chevrolet battery cooling(11)

Figure 8 shows the cooling system used by GM Chevrolet for their EV Bolt. In this system, each battery is connected to a cooling fin, which has engraved channel for coolant flow. This type of system is very reliable but much too costly to produce.

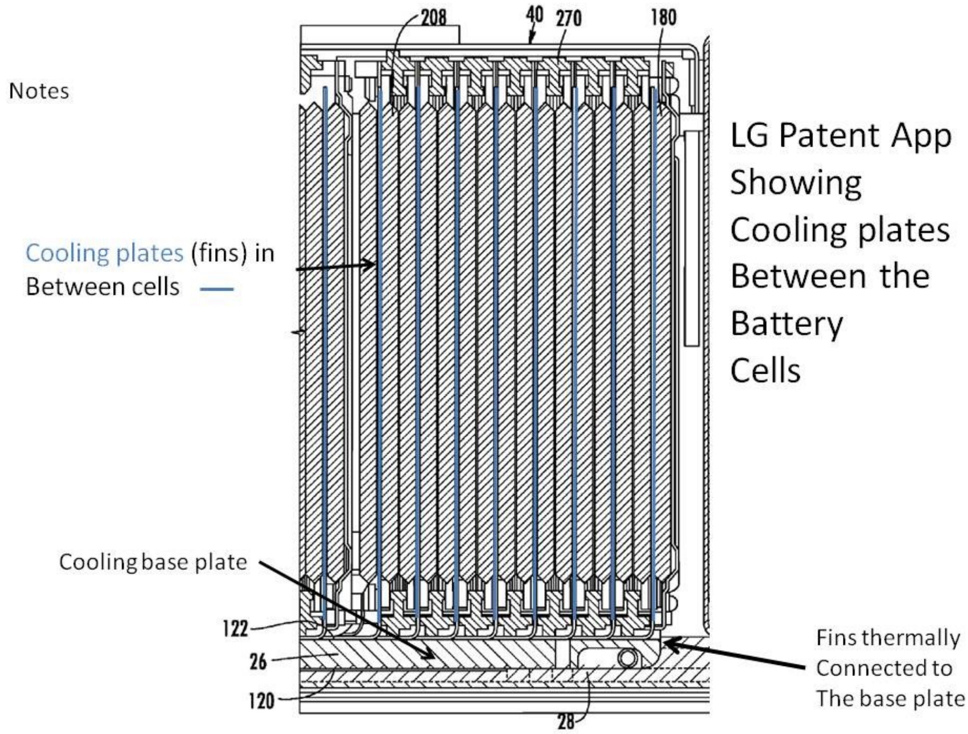

Figure 9 BMW cooling system(12)

BMW on the other hand has teamed up with LG to come up with a solution where refrigerant is used to provide Direct Expansion Cooling. Figure 9 shows the design of the system from the Patent application filed by LG. This is advantageous in many ways, but use of refrigerant is frowned upon because of its effect on Global warming.

Another new technique is being used, whether independently or in conjecture with the above technique, is the BCPs. The BCPs provide cooling to the base of the battery modules which helps to keep them in the optimal operating temperature. Figures below shows some examples of the BCPs currently produced and used. The technology used for manufacturing these BCPs are Milling or Copper tubing

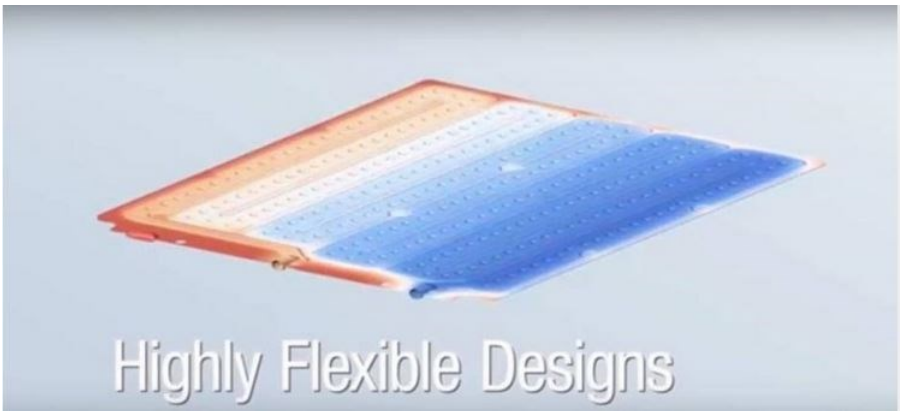

. **Figure 10 Dana Bottom cooling plate used by GM**

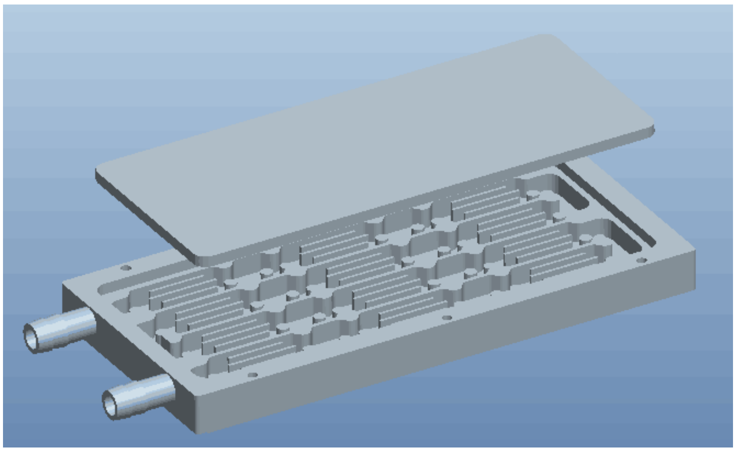

Figure 11 Bottom cooling plate by Walmate Thermal

3 Theory and Approach towards Modelling of Heat and Mass transfer

3.1 Introduction

This thesis makes use of commercial CFD software Fluent, developed by ANSYS Inc., to perform simulation of heat transfer and fluid flow in the BCP channels. In CFD; numerical analysis and data structures are used to simulate, analyze and solve problems in systems involving fluid flow (13). CFD can simulate and solve problems relating to Heat and Mass transfer, fluid flow characteristics, species diffusion, chemical reactions, Discrete Phase Modelling (DPM) and many more (14).

CFD softwares are used in many fields like aircraft industry, ship building industry, electronic engineering etc. to model flow of air, water or other medias over stationary or moving objects. CFD software coding is divided into three parts (13):

- Pre-processor – This deals with creation of geometry, assigning properties to materials and fluids, meshing, defining boundary conditions, defining the type of solver to use etc.
- Solver – This is the segment where the governing equations are solved.
- Post-processor – This is where the solutions can be viewed. Solutions can be viewed in form of contours, charts, graphs etc.

CFD softwares are very demanding on Computational resources. So a powerful computer was used to simulate the models. The specs of the computer is as follows:

Processors : Intel Xeon X5680 @3.33 GHz 2 core 24 thread processor.
GPU: NvidiaQuadro 4000
256 Gb SSD
2 Tb HDD RAID

In addition to this, since this thesis was completed in a short time, another less powerful computer was used to simulate model concepts with lower number of elements.

Processor: Intel Xeon E3-1231 Quad core@ 3.4 GHz
GPU: Nvidia Quadro K2200
256 Gb SSD
16 Gb RAM

For the more powerful computer, Double precision and 10 threads parallel processing was selected whereas for the less powerful computer, Double precision and 4 threads parallel processing was selected. GPUs were not utilized for the simulation processes:

3.2 Governing Equations

In the solver, which is Fluent in this thesis, the governing equations are integrated over all the control volumes (13). Then, Discretisation of the equations takes place and ultimately the algebraic equation derived in the Discretisation methods are solved in an iterative process.

In fluid and heat flow analysis, fluent solves the equations for conservation of Mass, Momentum and Energy.

The equations are presented below:

3.2.1 Mass conservation:

$$\frac{\partial \rho}{\partial t} + \Delta \cdot \left(\rho\vec{V}\right) = S_m$$

Where S_m is the Source term.

3.2.2 Momentum Conservation Equation

$$\frac{\partial}{\partial t}(\rho\vec{v}) + \nabla.(\rho\vec{v}\vec{v}) = -\nabla p + \nabla.(\bar{\bar{\tau}}) + \rho\vec{g} + \vec{F}$$

3.2.3 Energy conservation equation

$$\frac{\partial}{\partial t}(\rho E) + \nabla.\left(\vec{v}(\rho E + p)\right) = -\nabla.(\sum_j h_j J_j) + S_h$$

When the Calculate button is pressed in the Fluent solver, fluent tries to solve the above equations for the heat and mass transfer. The end form of the equations depends on the type of flow. For inviscid flows, it approaches the Eulerian equation.

3.2.4 K-ε turbulence modelling

Additionally, in Fluent, K-ε wall function model can be used to model the turbulent flow. In this case, the equations for solving the model are computed as below:(15)

K is computed from:

$$G_k \approx \tau_w \frac{\partial U}{\partial y} = \tau_w \frac{\tau_w}{\kappa \rho C_\mu^{1/4} k_P^{1/2} y_p}$$

and ε from the equation:

$$\epsilon_P = \frac{C_\mu^{3/4} k_p^{3/2}}{\kappa y_P}$$

The k-ε equation is used to solve the heat transfer problem as part of the Scalable and Realizable wall function model. The turbulent intensity and the Turbulent dissipation rate which the k and ε denotes, provide a very important insight into the flow in the near wall region. The Scalable wall function is used at y*<11.5, so it is more reliable than its counterpart, Standard wall function

4 Material Properties

The material used in this thesis are listed below.

Table 1 Material Properties

Material/Properties	Copper	Aluminum	Water
Thermal cond.(W/m K)	401	202	0,58
Density(kg/m^3)	8960	2700	998
Cp (J/K)	385	900	4178
Thermal Diffusivity	0.00016	0.000083	0.000000139
Thermal Effusivity	37192.675	22155.360	1555

It is seen from the above table that the Thermal effusivity of Copper is higher than Aluminum, which is in turn higher than that of Water. Thermal effusivity is the easiness with which a material dissipates heat to its surrounding bodies. In the HFSC technique, Copper is connected thermally to Aluminum, which is in turn connected to Water. This gradient in thermal effusivity among the three components, makes it possible to have a smooth and efficient heat flow from copper into water through the aluminum.

Another reason copper was chosen was because of its very high thermal conductivity. In the HFSC arrangement discussed later, copper is mainly used for transferring the heat from the battery into the Aluminum plate. Another reason copper was chosen was because it is possible to get uniform temperature along the coper surface in a very short time as copper dissipates heat faster due to the superior thermal properties.

5 Modelling Conditions and Pre-Processing

5.1 Component models

Models were designed using commercial CAD software CREO Parametric They were then imported into DesignModeller as .STP files and the fluid domains created. The different models are shown below.

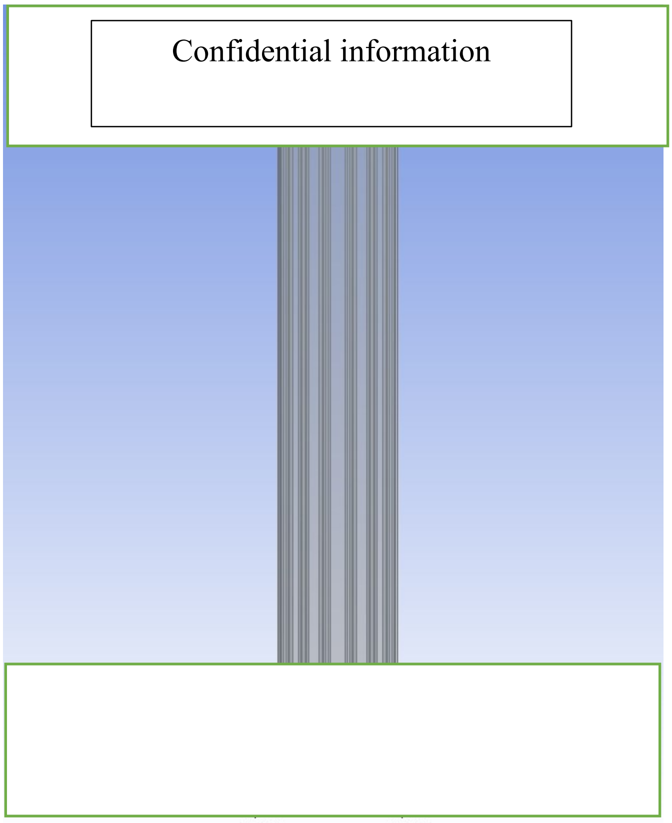

Figure 12 Milled and FSC model

The model in the figure above consists of an aluminum base plate and a channel inside it. The channel path was taken arbitrarily to provide maximum surface coverage.

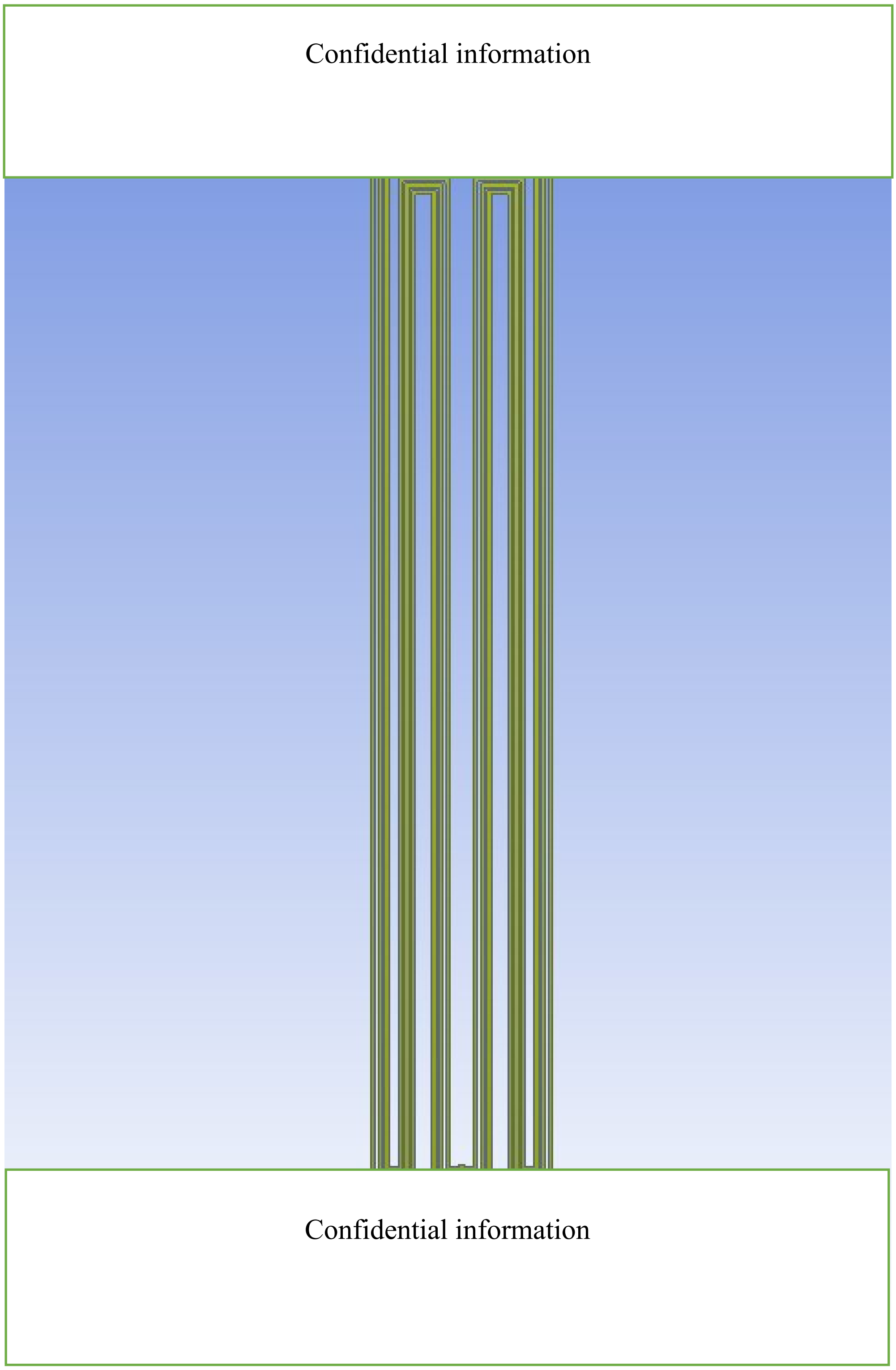

Figure 13 Fluid channel for Milled and FSC

The figure above shows the fluid domain of the model used in the Milled and FSC simulations.

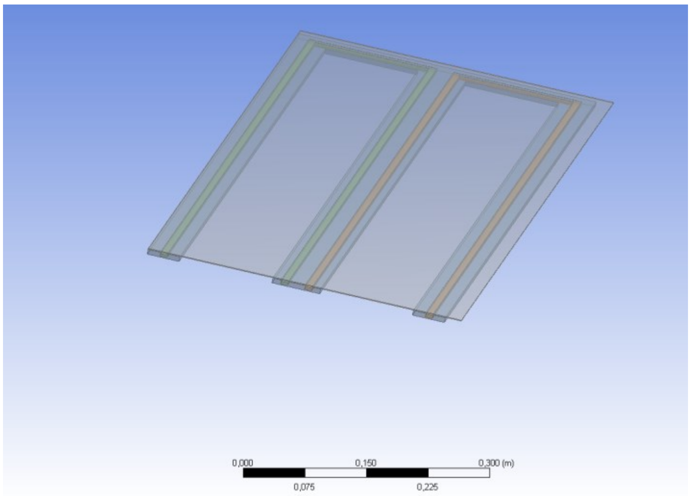

Figure 14 HFSCmodel 9

HFSC model 9 has a copper plate on top,1 mm thick, and an aluminum conformal cooling channel underneath. The fluid domain can be seen in the figure above.

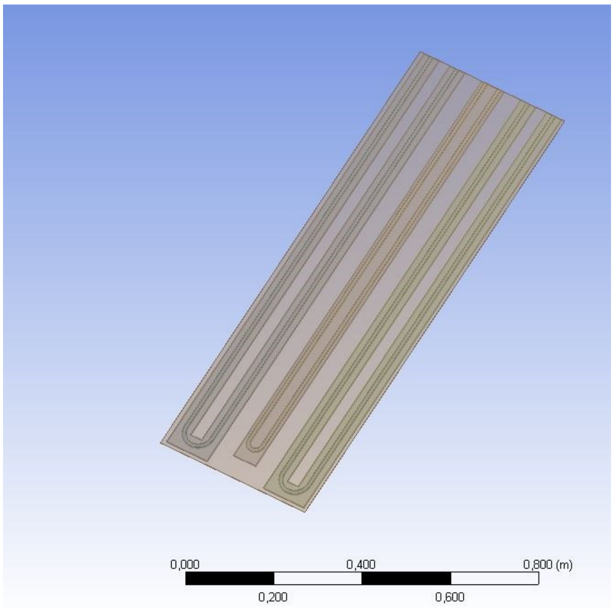

Figure 15 HFSC model 10

HFSC model 10 consists of 3 separate conformal cooling channels. This model was developed for ease of creating the aluminum plate from blocks of aluminum without any wastage. The copper on top is 1 mm thick, the aluminum plates are 6 mm thick.

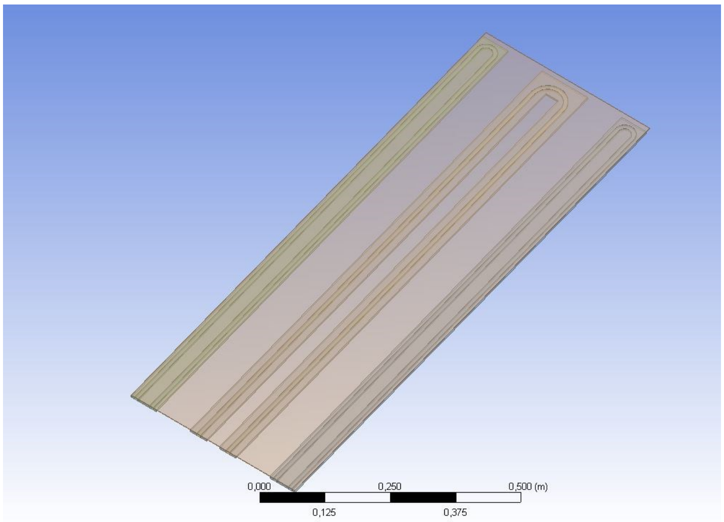

Figure 16 HFSC model 13

Figure 15 shows the model 13 of HFSC iterations. In this, 3 separate channel paths were created with the middle one being a conformal cooling channel. Like in the other cases, the top copper base plate is 1mm thick and aluminum plates each 6 mm thick.

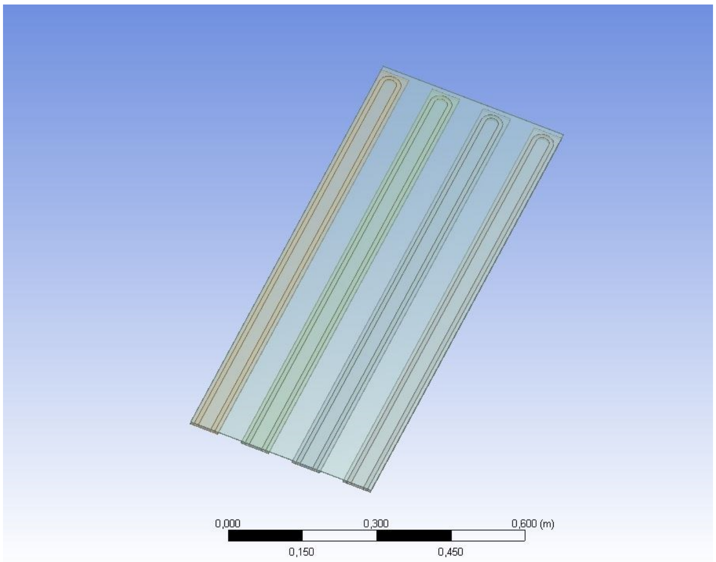

Figure 17 HFSC model 14

HFSC model 14 consists of four 60 mm wide conformal cooling channels. The aluminum plates are 5 mm thick and the copper plate 1 mm thick.

5.2 Mesh statistics

The mesh statistics for each model are as follows

Table 2 Mesh statistics

Model	Number of elements	Mesh type	Element size(m)
Milled and FSC	7373148	Fine,Proximity curvature	Min size $1x10^{-5}$
HFSCmod9	8913867	Fine,Adaptive	$5x10^{-4}$
HFSCmod10	10822130	Fine Adaptive	$5x10^{-4}$
HFSCmod13	10262589	Fine Adaptive	$5x10^{-4}$
HFSCmod14	1163653	Fine Adaptive	$5x10^{-4}$

5.3 Boundary and initial conditions

Boundary conditions were put in for each model. Mostly the boundary conditions are same. Thermal load in form of Heat flux was placed on the top face of aluminum in case of Milled and FSC, and top face of copper plate in case of HFSC models. The heat flux represents the heat that is given into the system. The heat flux was calculated from the internal resistance to be a total of 3.7 kW/m^2, but to push the models further and get a good safety margin, the heat load was input as 4.5 kW/m^2 .

The interface between the separate parts in the assembly were set as Coupled wall for heat transfer between them. The interface between the fluid domain and the aluminum was also set as a coupled wall. All the other walls in the system was treated as an adiabatic wall. For the roughness model, the equivalent sandgrain roughness height was calculated using the formula:

$$\varepsilon = 3.100 R_{RMS} \quad \textbf{(16)}$$

where ε is the equivalent roughness height and Rrms is the Root mean square value of the Roughness height. The Rrms value was taken from unpublished article of Karvinen et al(17). The calculated roughness value was then input into the boundary interface between the water and the aluminum surface. It is to be noted that the roughness introduced is only simulated roughness and not real roughness.

Symmetry boundary conditions were used on the HFSC models to make them smaller in size.

All the componets were given an initial temperature of 298.15 K. The inlet for the fluid was set as a Velocity inlet with a flow rate of 1 m/s. The outlet was set as Pressure outlet at atmospheric pressure.

The solver used was a Pressure based segregated solver. Segregated solver was preferred over Coupled solver because of the processing power limitations. k-ε wall function was used with Scalable and Realizable wall function.

6 Model Validation

6.1 Experimental Setup

The experiment was conducted on a FSC sample prepared for this validation. The sample is shown in the figure below

Figure 18 Test sample

The sample was 190 mm long and 105 mm wide. Couplings were fitted on the end of the sample for fluid flow and inlet and outlet pipes were attached. The sample was then fitted with thermocouple and placed in a insulated box.

Figure 19 Insulated box

This box was also fitted with thermocouples to notice the temperature changes. The thermocouples were then fitted to Graphtec Midires datalogger. The box was filled with 10L of water at 52 degree temperature. Then water at 21 degree C was made to flow through the sample after closing the lid of the box. Water was pumped in at 0.4 bar pressure and outlet was noted to be at 0 bar pressure. The setup was kept closed until the datalogger showed that the sample has reached a steady state. 4 more tests were done at different temperatures and the data was logged.

To test the simulation validation, a CREO model of the sample was created along with the couplings. Figure below shows the CAD model.

Figure 20 CAD model of the sample

The model was then meshed and loaded into fluent solver. Transient analysis was performed on the sample to validate the data. Pressure was noted as well to further validate the model.

The validation couldnot be completed on time and will be continued after this thesis.

7 Case studies

In this section, the BCPs made by the different methods are compared to each other. In the first subsection, Results, individual results are shown. In the next section, Comparison, the comparison between Milled and FSC channels are showed first. Then they are compared to the HFSC models. Different criteria for comparing the result were also included in this subsection.

It is also to be noted that, to maintain uniformity in comparison, the section of the baseplate that is in contact with the battery modules are compared to each other. In the case of Milled and FSC plates, it is the top surface of the aluminum plate, and in case of the HFSC models, it is the top surface of the copper plate.

Throughout the course of the thesis work, it was understood that simulation can not be as perfect as experimental work. But the results from the simulations, whether perfect or not, gives an idea about whether the concepts are worth working on. This saves time and money spent on building and testing real life models, which is impractical in most cases.

In this thesis work, a lot of effort were put into design and simulation of new concepts, which could ideally show better heat and mass flow characteristics than what, is traditionally used. In total, 1 Milled model, 1 FSC model and 14 HFSC models were simulated. Out of the 14 HFSC models, 4 models were selected which showed promise for further development. In the following chapters, the results and comparison between those models are detailed.

7.1 Results

7.1.1 Milled channel

For milled channel, the roughness of the interior was set to 0 to simulate smooth surface. Then the heat flow and fluid flow were simulated as mentioned in the previous **chapter.** To get more accurate result, the convergence criteria for the residual monitors were set to $1\text{x}10^{-4}$ except for the energy monitor, which was set to $1\text{x}10^{-6}$. This leads to longer time taken for the solutions to converge, but gives a much more accurate result. The residuals plot and convergence can be seen below.

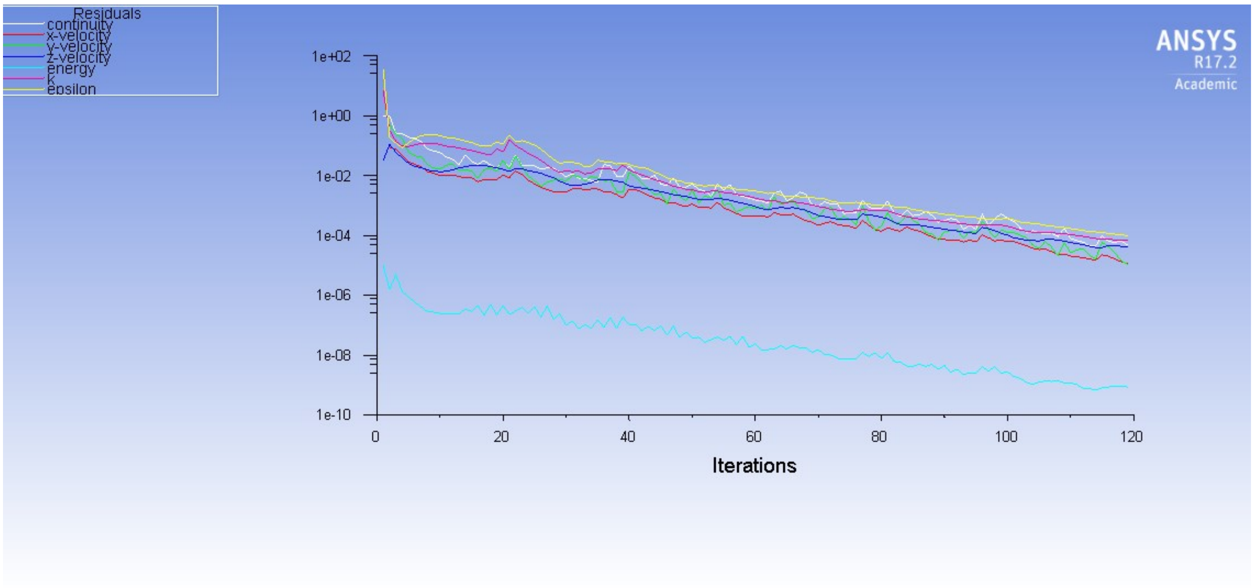

Figure 21 Residuals for Milled simulation

```
!  119 solution is converged
   119  4.8967e-05  1.1316e-05  1.0989e-05  4.0752e-05  8.6947e-10  6.9036e-05  9.9893e-05 30:52:19 4881
```

Figure 22 Convergence

7.1.2 FSC

For the FSC channel, the roughness value was taken as equivalent sand-grain roughness with Roughness height 0.0018 m. In this case as well, the convergence criteria was set to be $1x10^{-4}$ for all the convergence monitors, except for energy, which was again taken to be $1x10^{-6}$. The residuals plot and the convergence point is shown in the figure below.

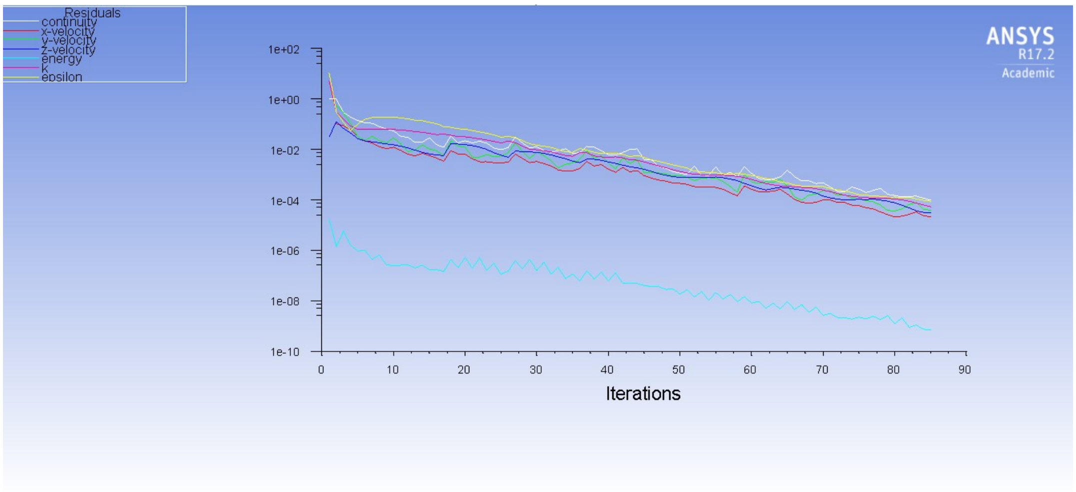

Figure 23 Residuals for FSC

```
!   85 solution is converged
    85  9.7294e-05  2.1171e-05  3.8931e-05  3.1073e-05  7.3100e-10  5.3151e-05  8.8513e-05 34:55:39 4915
```

Figure 24 Convergence

7.1.3 HFSC models

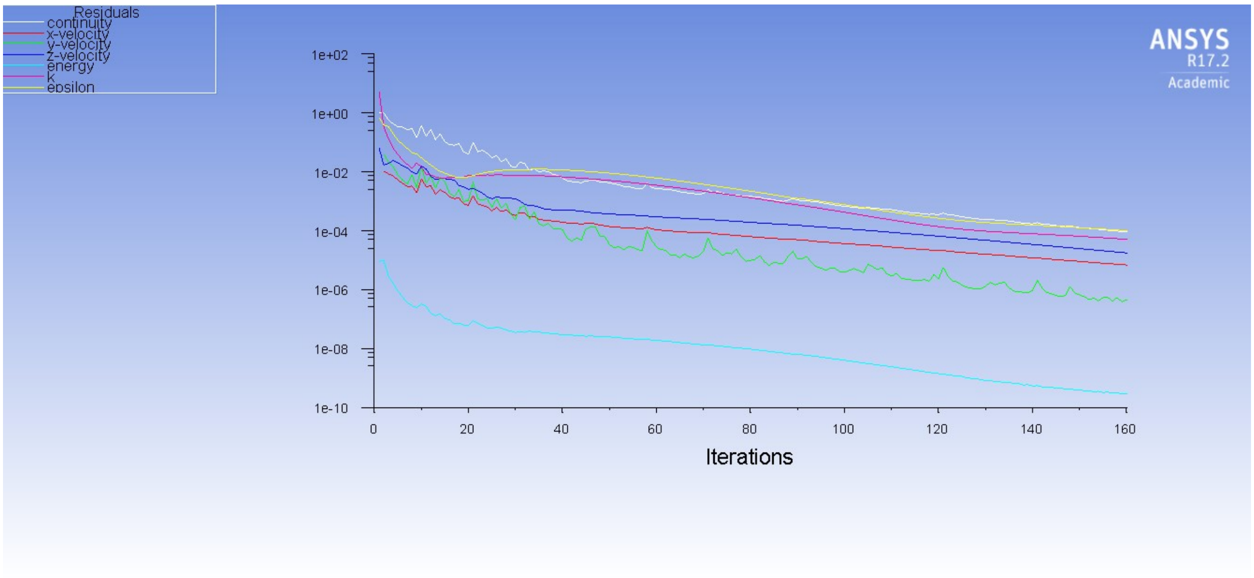


```
!  160 solution is converged
   160  9.1468e-05  6.8751e-06  4.4590e-07  1.7728e-05  2.9640e-10  5.1256e-05  9.9969e-05 25:08:58 4840
```

Figure 25 Residuals and convergence for HFSC model 9

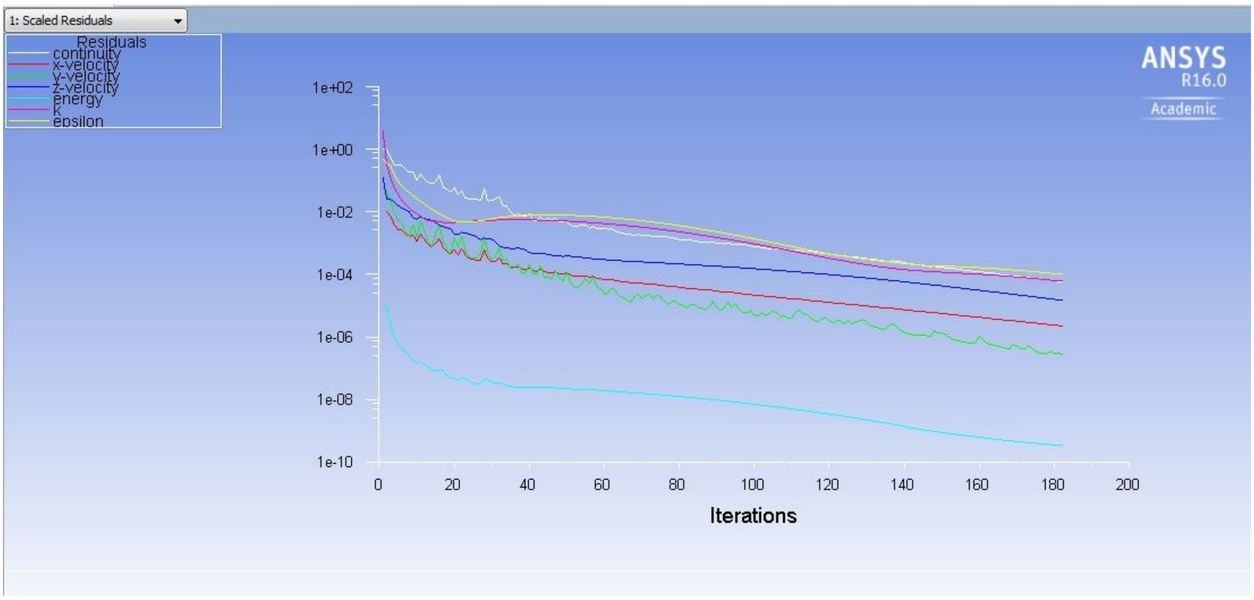

```
! 182 solution is converged
  182  5.7326e-05  2.2547e-06  2.8028e-07  1.4746e-05  3.3377e-10  5.9955e-05  9.8917e-05 19:20:01 4818
```

Figure 26 Residuals and convergence for HFSC model 10

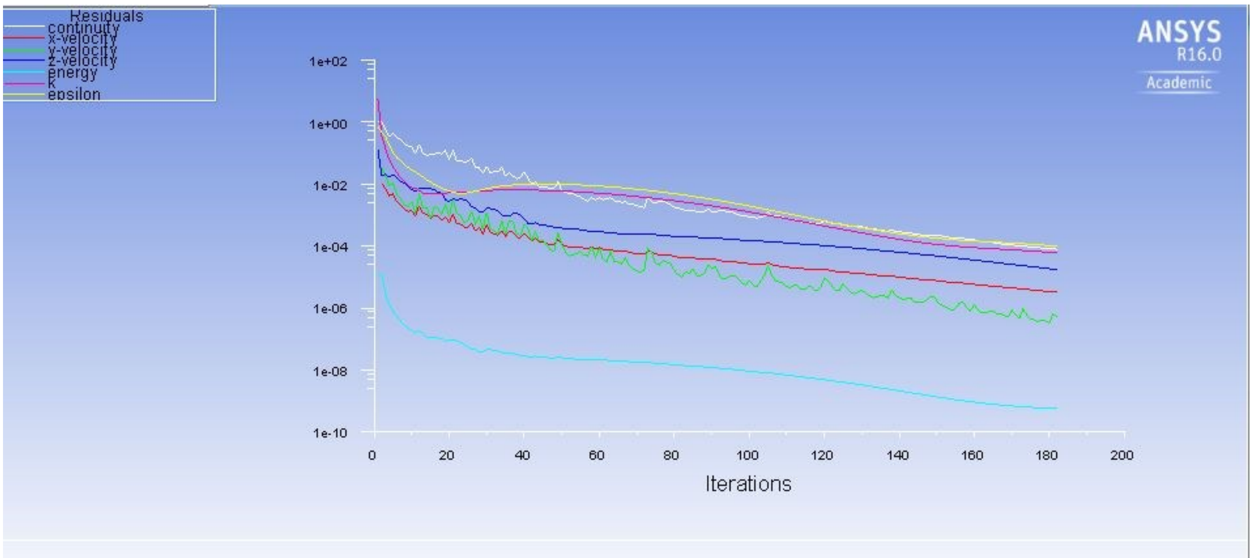


```
! 182 solution is converged
  182  7.8141e-05  3.3004e-06  5.3540e-07  1.7452e-05  5.6970e-10  6.0588e-05  9.9713e-05 18:15:52 4818
```

Figure 27 Residuals and convergence for HFSC model 13

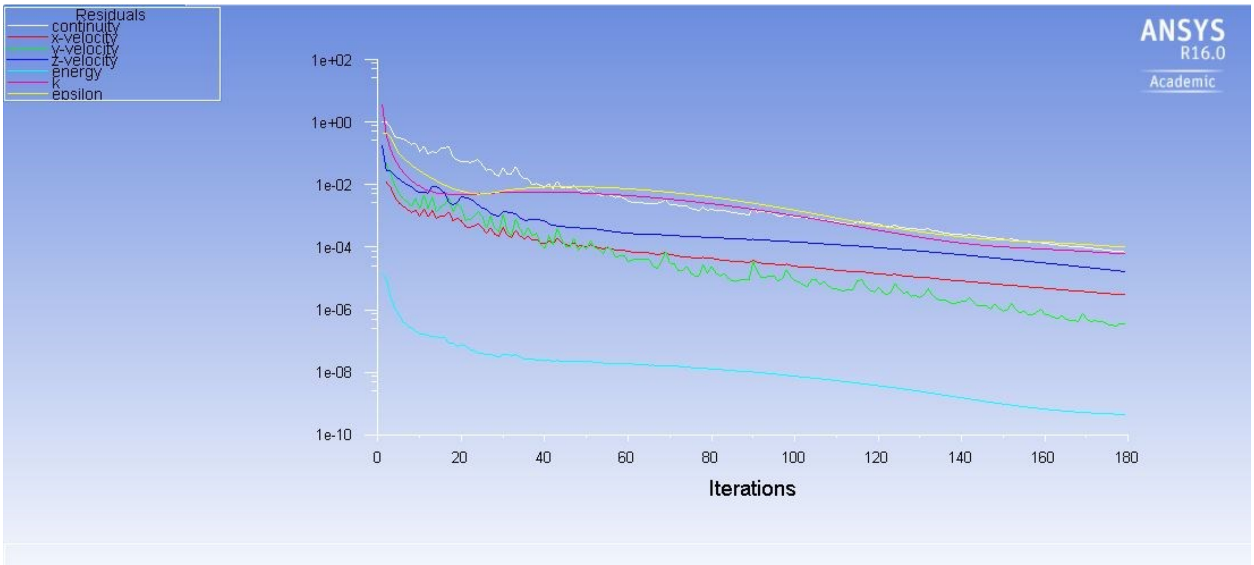


```
! 179 solution is converged
  179  7.0546e-05  2.9810e-06  3.5802e-07  1.6701e-05  4.4641e-10  5.9894e-05  9.8767e-05 21:55:56 4821
```

Figure 28 Residuals and convergence for HFSC model 14

A very low convergence criteria gives a more reliable result, so 1×10^{-5} was selected.

7.2 Comparing the Models

This section deals with comparing the Milled, FSC and HFSC models. First, the Milled and FSC models are compared to see if the roughness introduced in the FSC plate causes any noticeable changes. It can be recalled that the only difference between the Milled and the FSC model was the introduction of roughness height on the channel surface. So, any difference observed will directly be a result of the roughness in the channel which is caused during the FSC process.

7.2.1 Milled vs FSC

Temperature variation Across Line 1

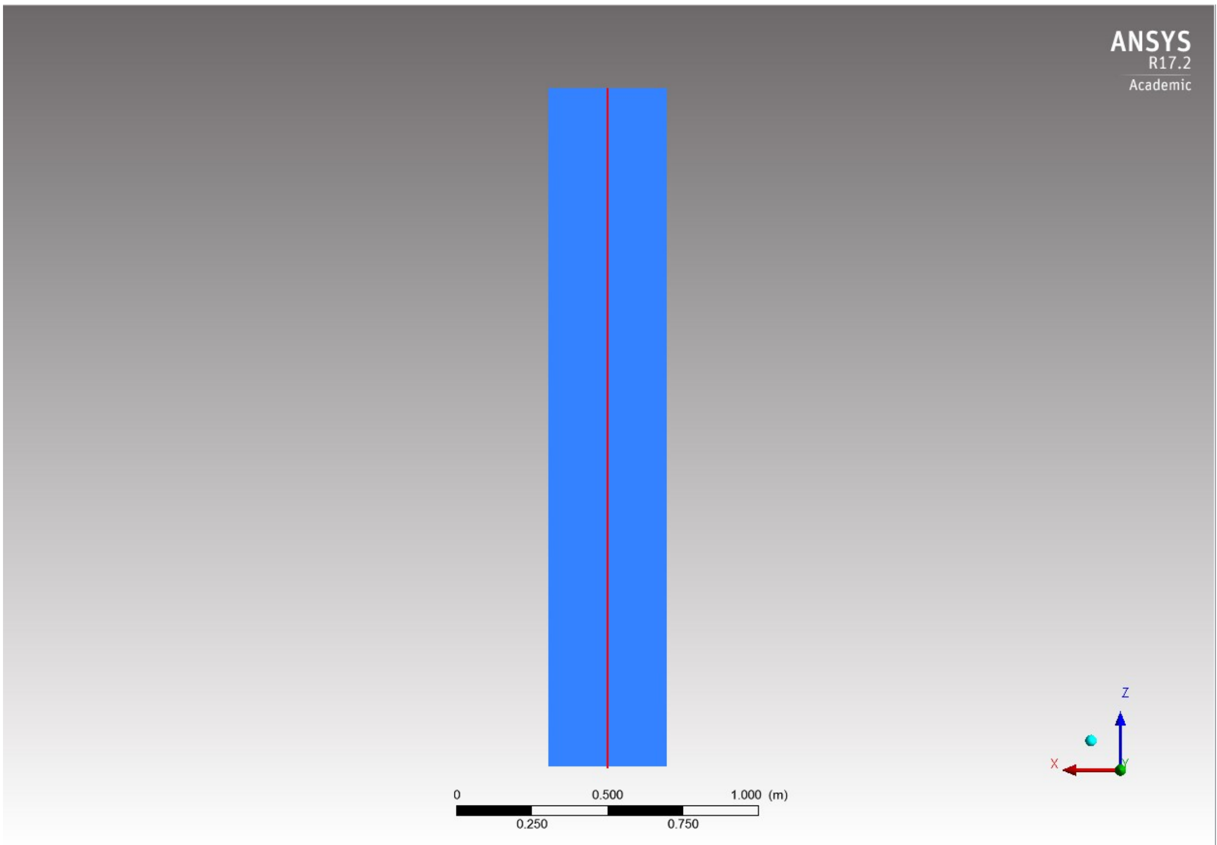

Figure 29 Location of Line 1

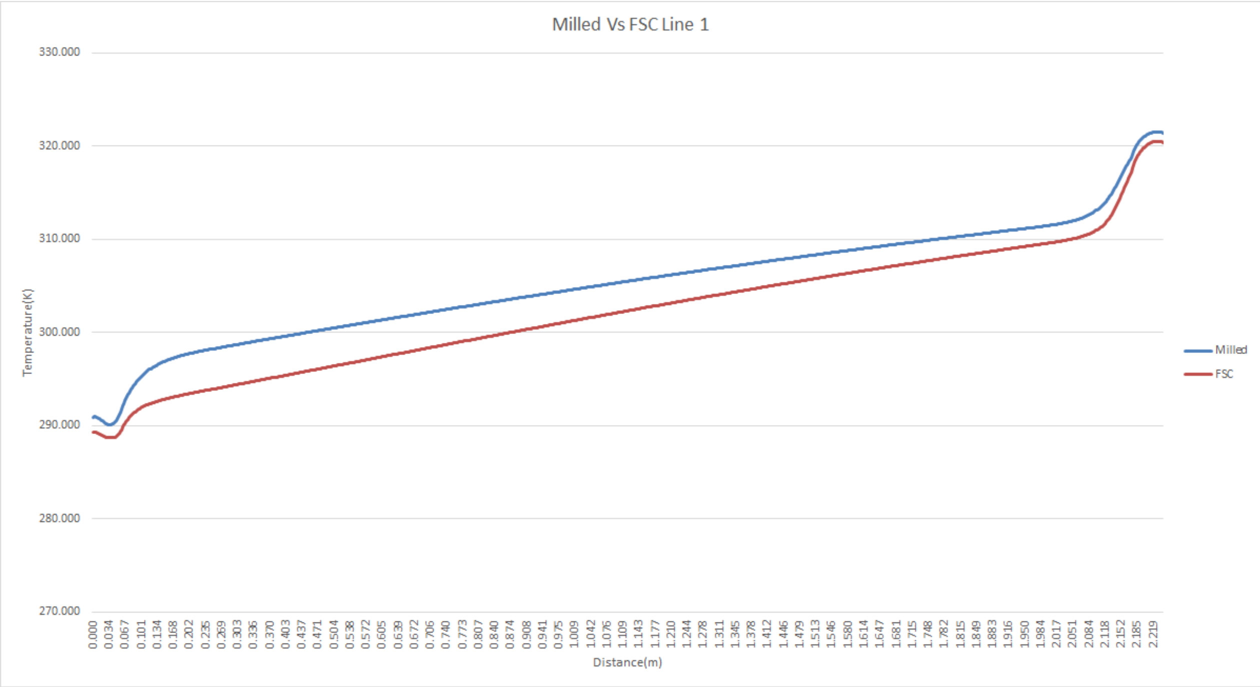

Figure 30 Milled vs FSC line 1

Temperature variation Across Line 1

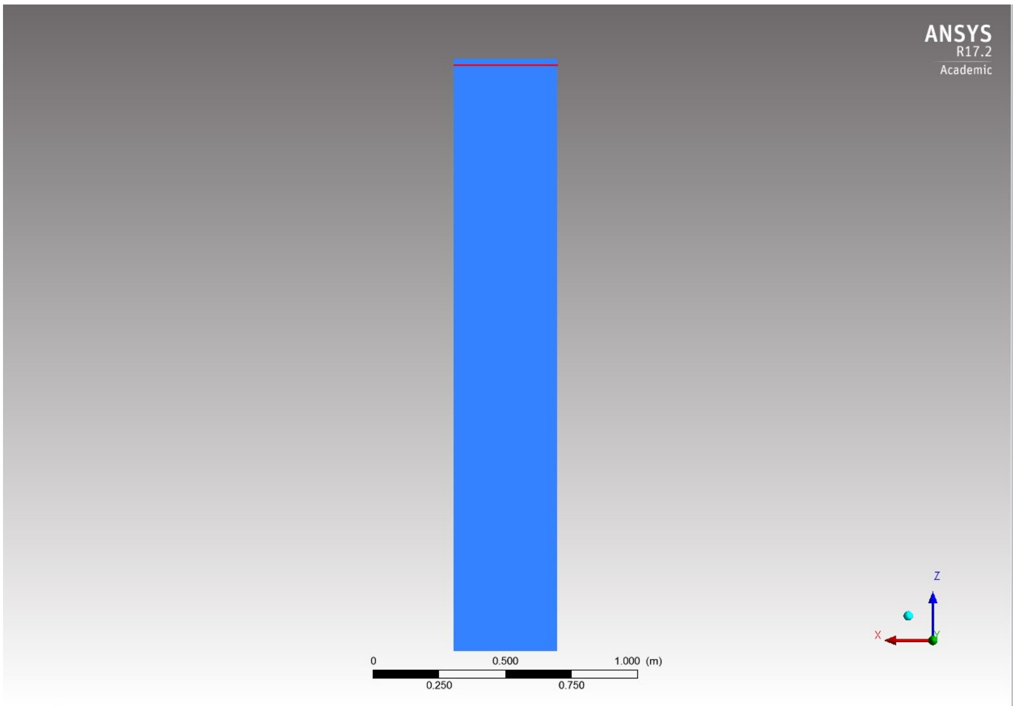

Figure 31 Location of Line 2 at the top of the plate

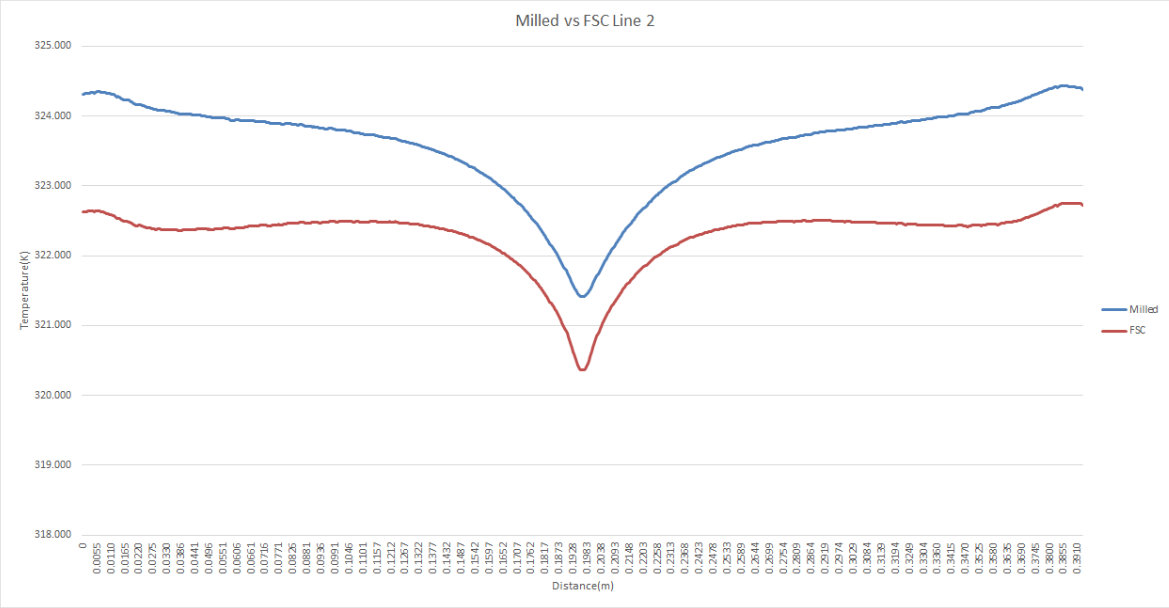

Figure 32 Milled vs FSC line 2

Temp variation across Line 3

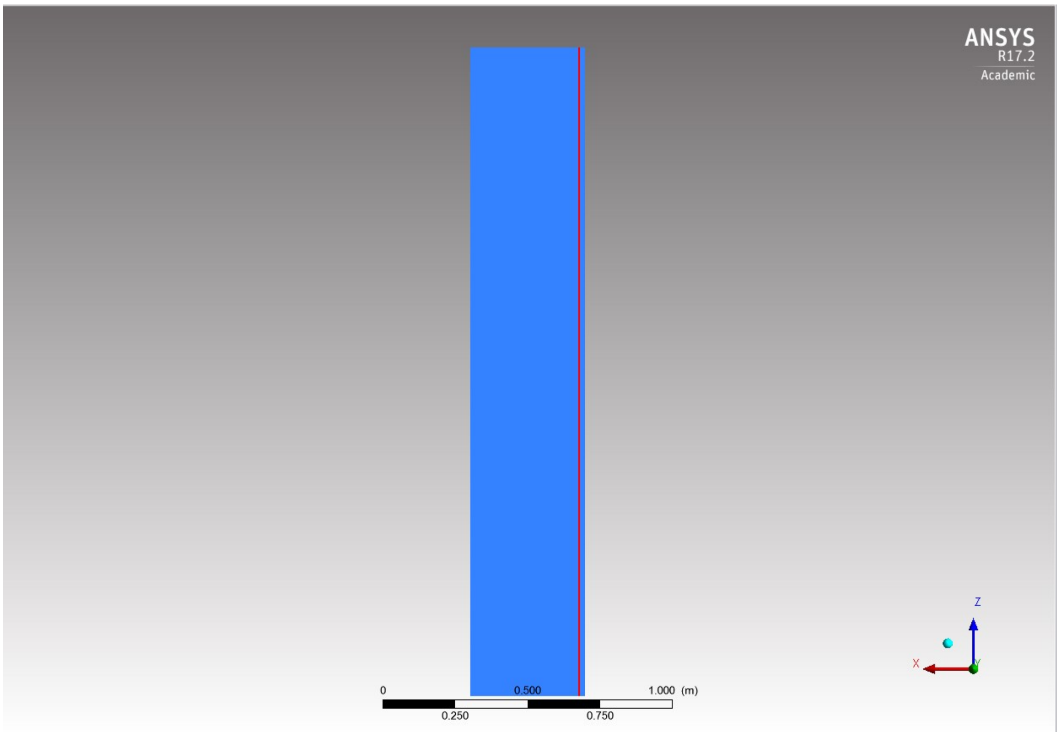

Figure 33 Location of Line 3

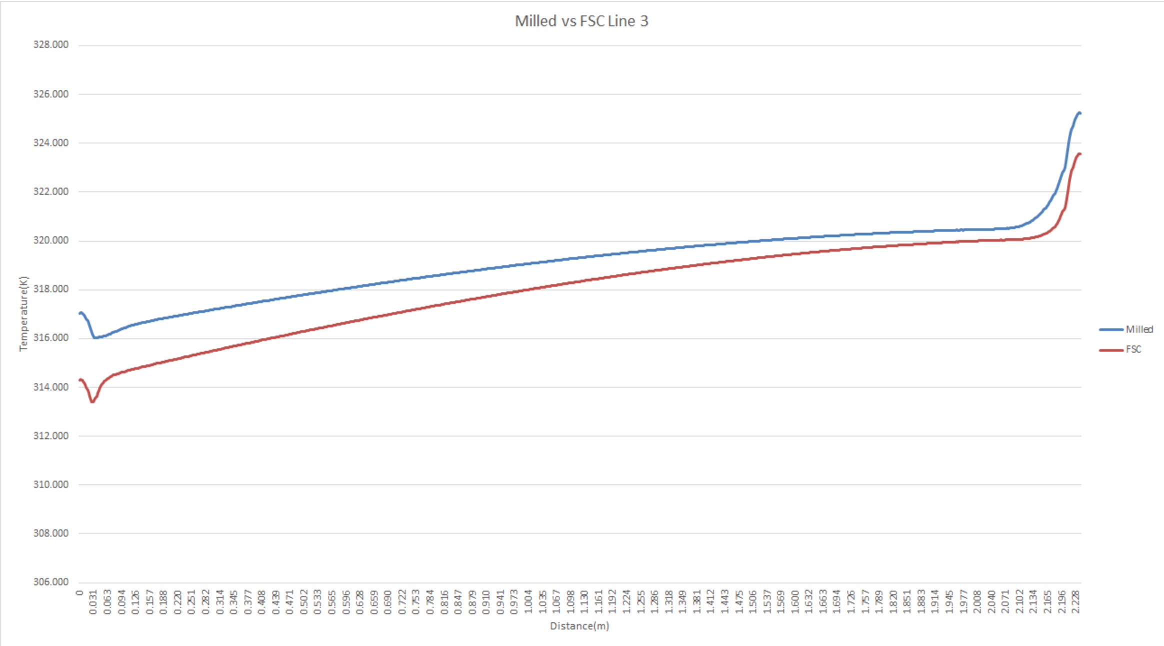

Figure 34 Milled vs FSC line 3

From the above figures, it can be seen that the temperature in the FSC plate at the same position is lower than that of Milled channel. Only difference between these two models was the introduction of Roughness height. So, it can be said from the pictures that roughness introduced cause the drop in temperature. This can be attributed to the fact that the roughness caused turbulent flow in the channels, which in turn helped in bringing down the temperature.

7.2.2 Milled vs FSC vs HFSC

Now that it has been seen that the roughness introduced indeed causes a difference in the thermal capabilities, further comparison of the Channels can be done with the HFSC models. From these comparisons, it is desired to be seen if the introduction of the copper plate for its superior thermal properties causes any noticeable change.

It can be noted that the HFSC models uses much less materials than their Milled and FSC counterparts. The reason for this comparison is to see if the introduction of copper allows for usage of much less materials in the assembly, since the aim is to reduce the weight and cost as much as possible.

Temperature contours

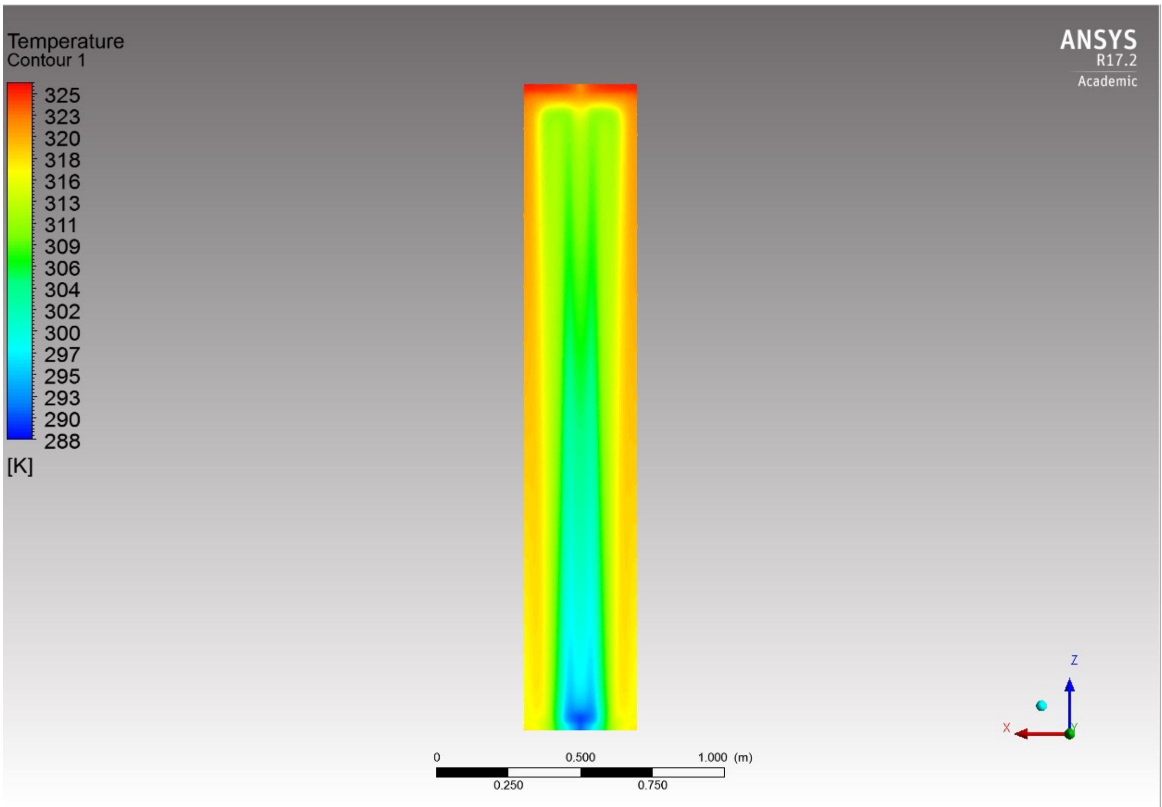

Figure 35 Milled temp contour

The milled temperature contour shows hot spots near the end on the sides. The maximum temperature of this sample was found to be 324K.

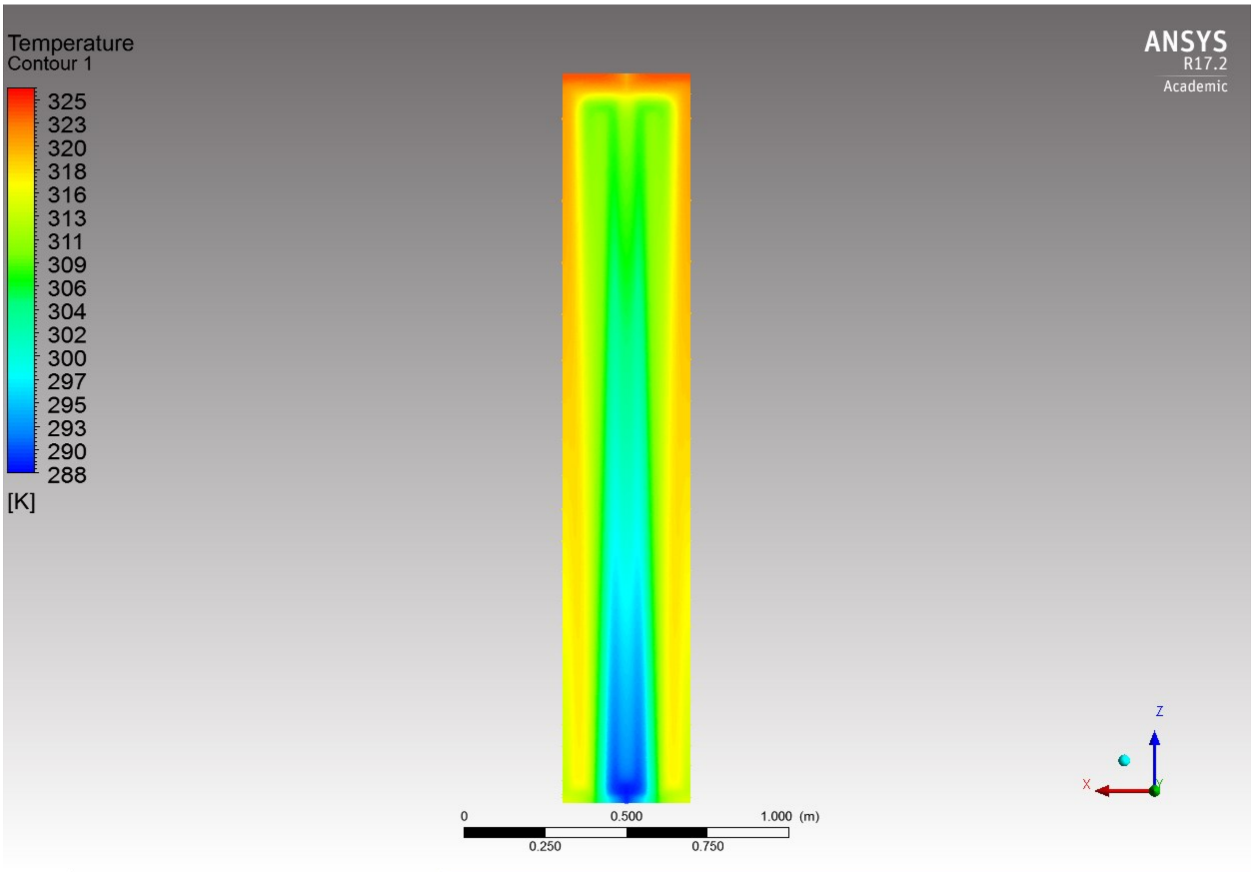

Figure 36FSC temperature contour

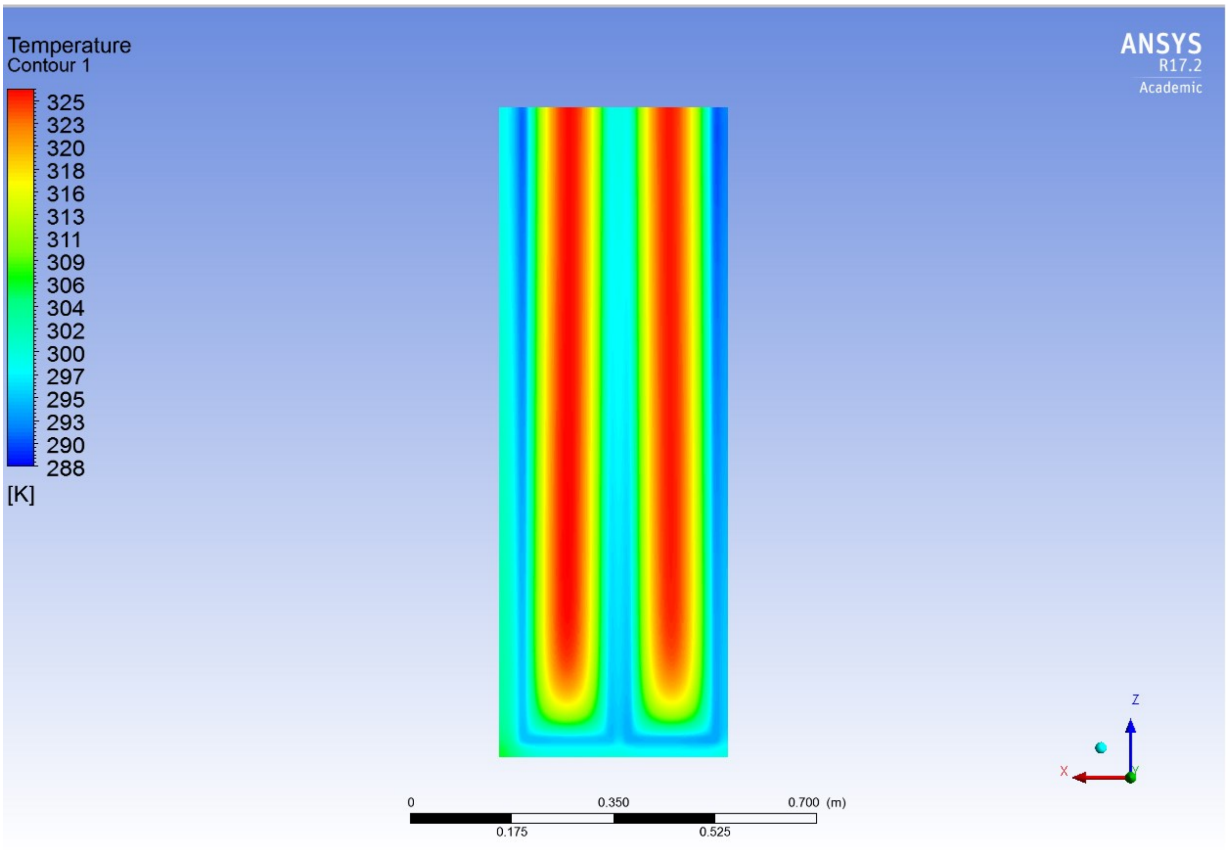

Figure 37 HFSC model 9 temperature contour

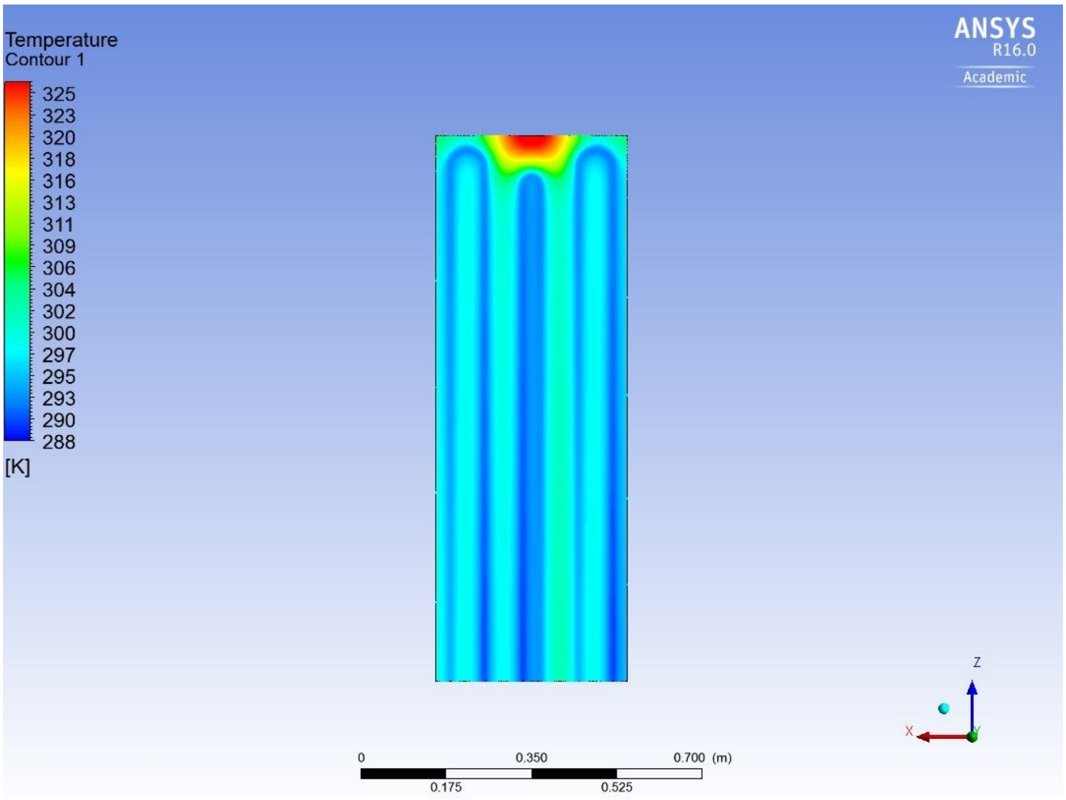

Figure 38 HFSC model 10 temperature contour

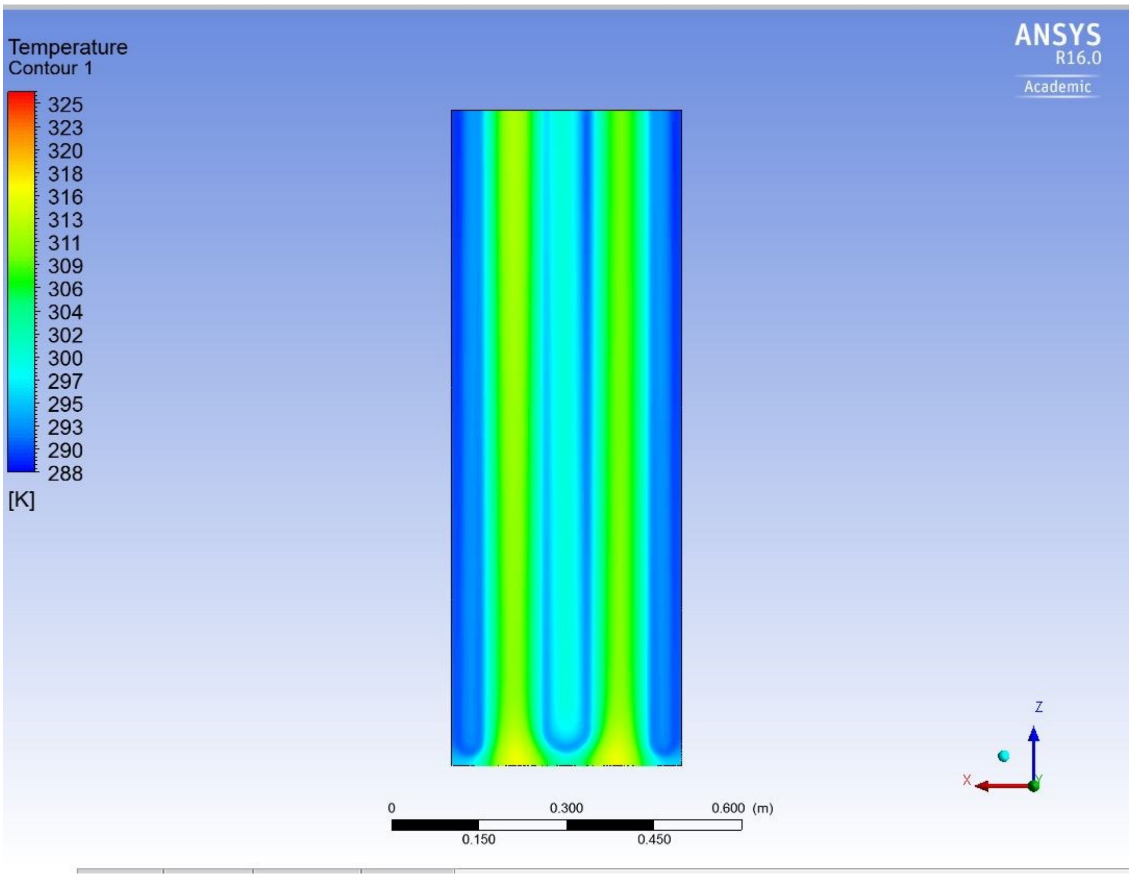

Figure 39 HFSC model 13 temperature contour

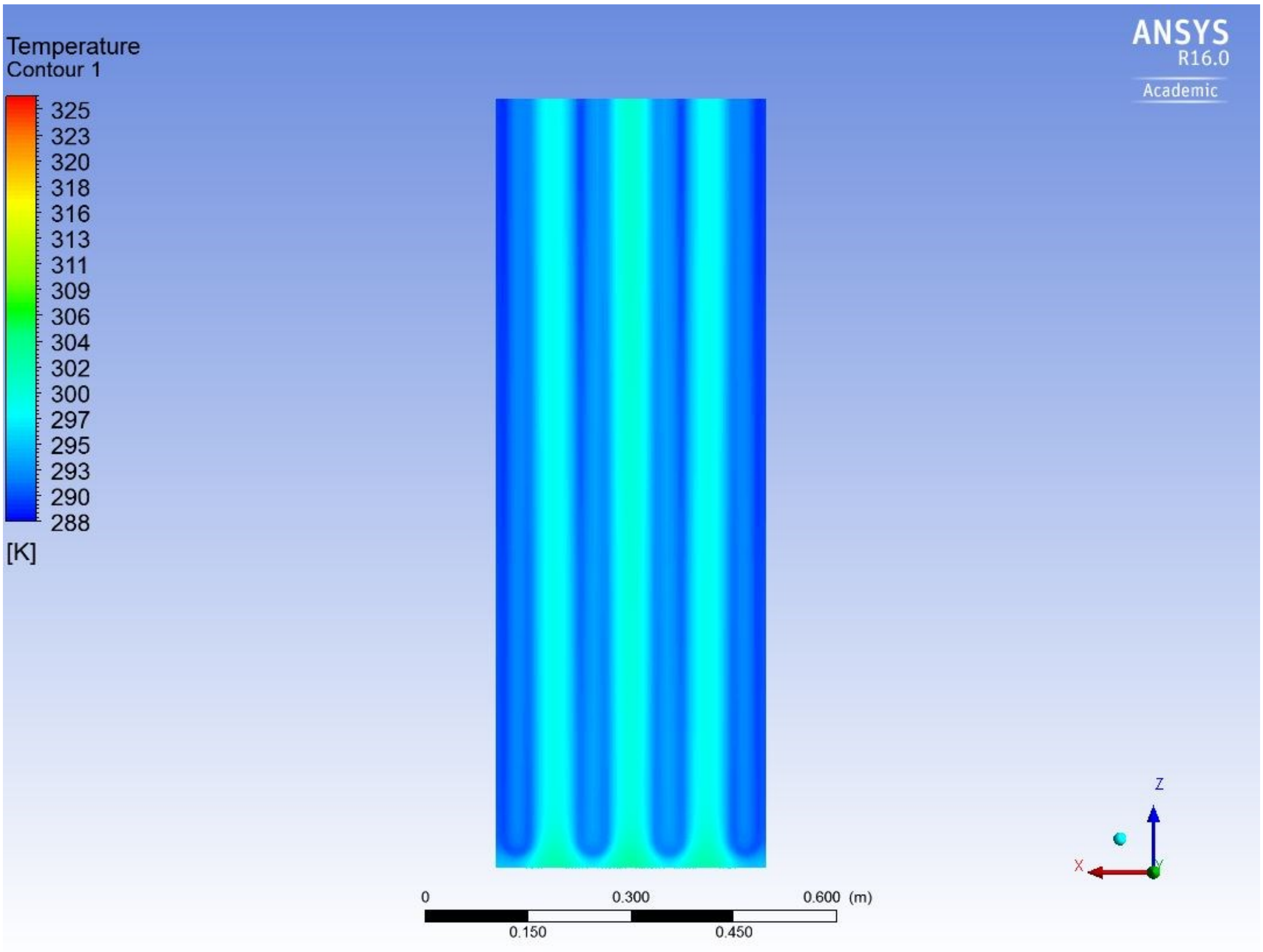

Figure 40 HFSC model 14 temperature contour

From the pictures of the temperature contours over the top of the base plate, it can be seen that HFSC model 14 was the best performing among the HFSC models. The maximum temperature in the HFSC model 14 was only 302 K. But before a model is selected for further development, the temperature variations can be looked at.

Temperature variation along the lines.

Across Line 1

Figure 29 Location of Line 1 shows the position of Line 1. For the HFSC models, it was also at the middle of the plate going from one long end to another.

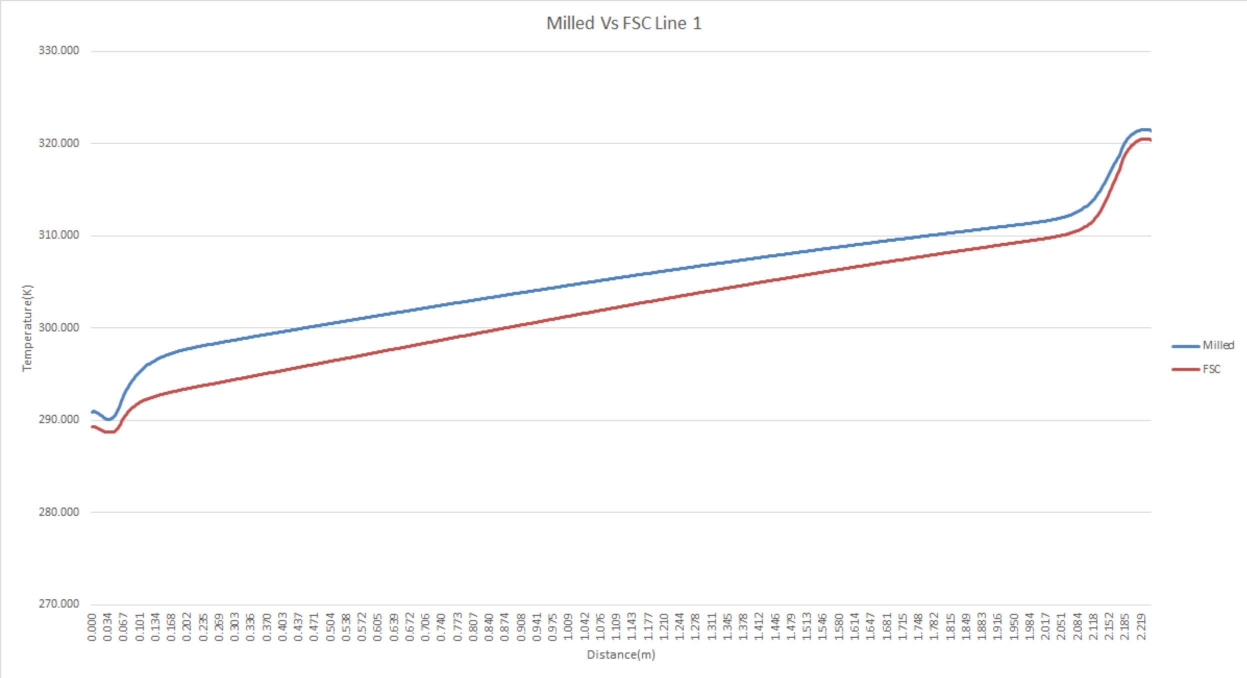

Figure 41 Milled vs FSC

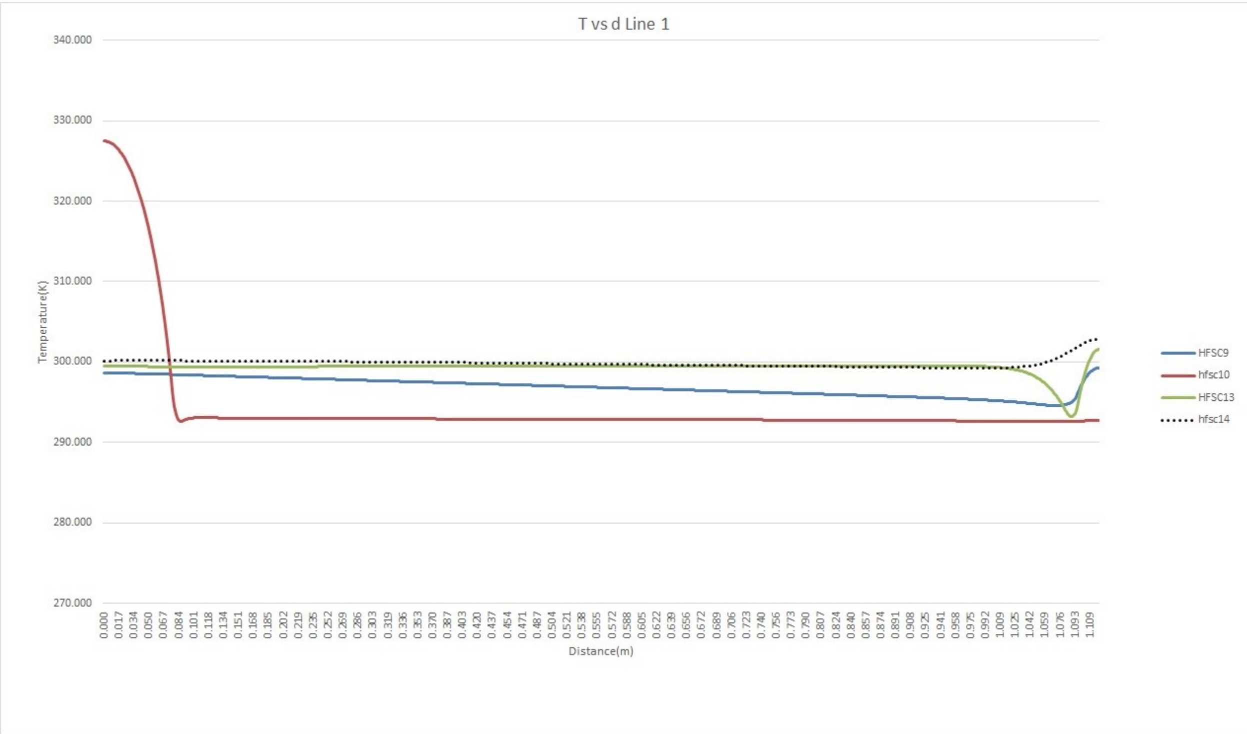

Figure 42 HFSC models

Across Line 4

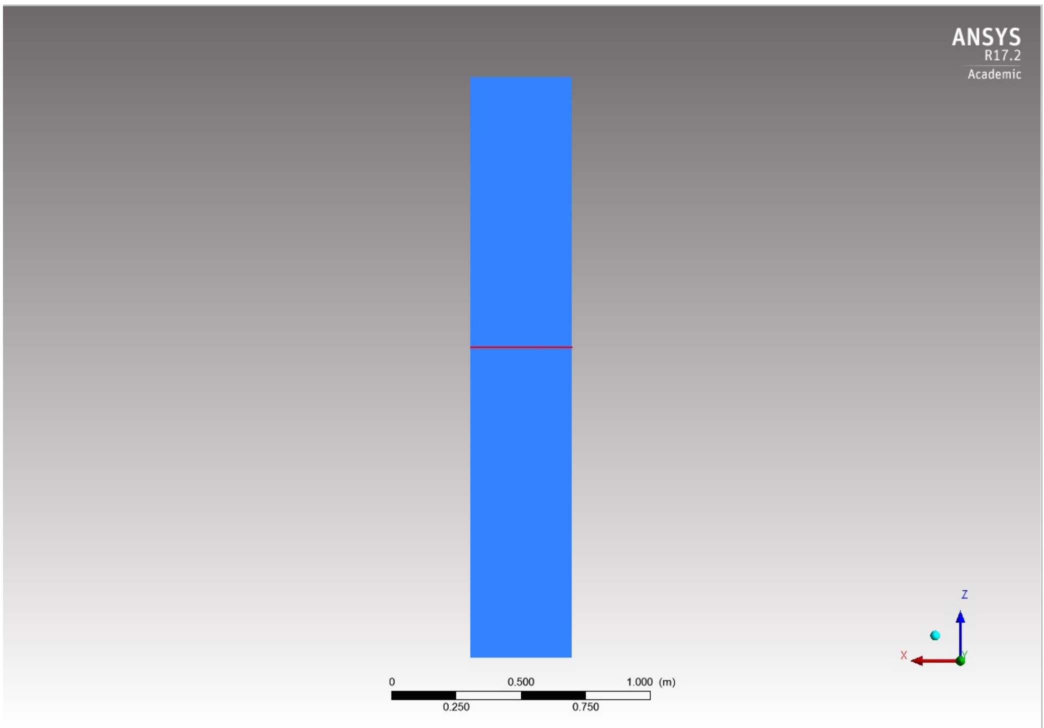

Figure 43 Location of Line 4

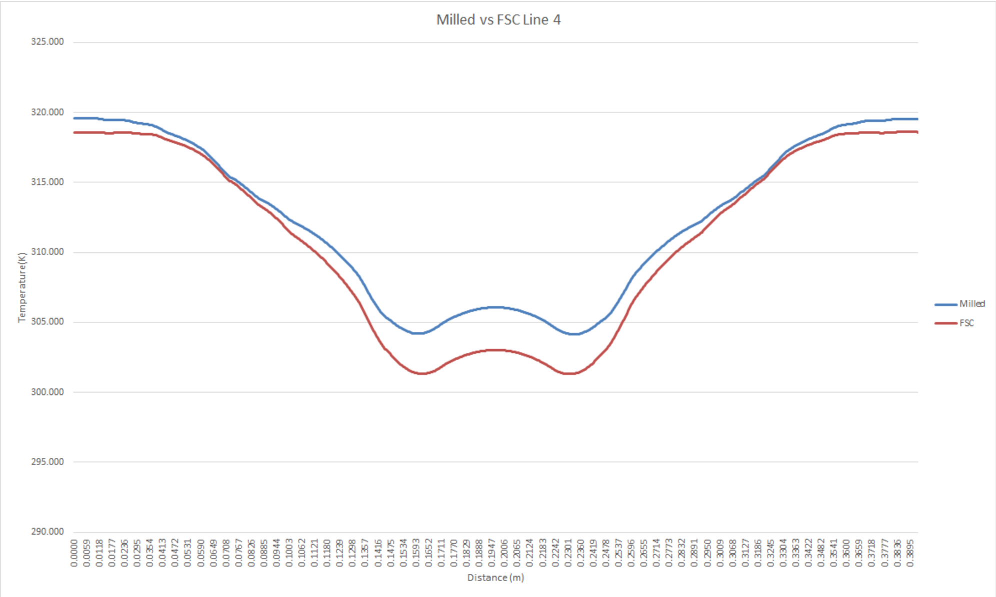

Figure 44 Milled vs FSC

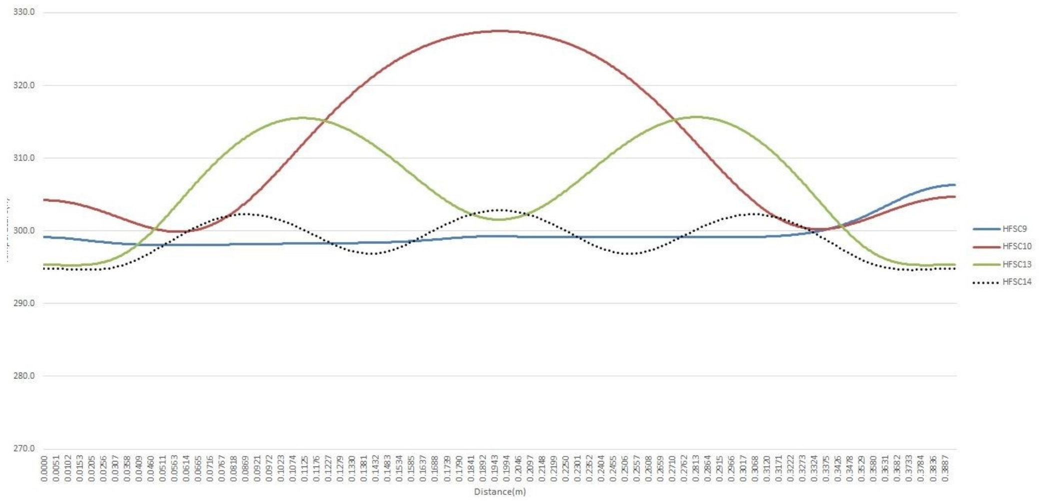

Figure 45 HFSC models

It can be seen from the above figures again that the HFSC model 14 maintains almost same temperature along the length and breadth of the plate.

Pressure Profile

The pressure profile of the Milled, FSC and HFSC models are shown below. The pressure profile shows regions of high pressure in the HFSC models.

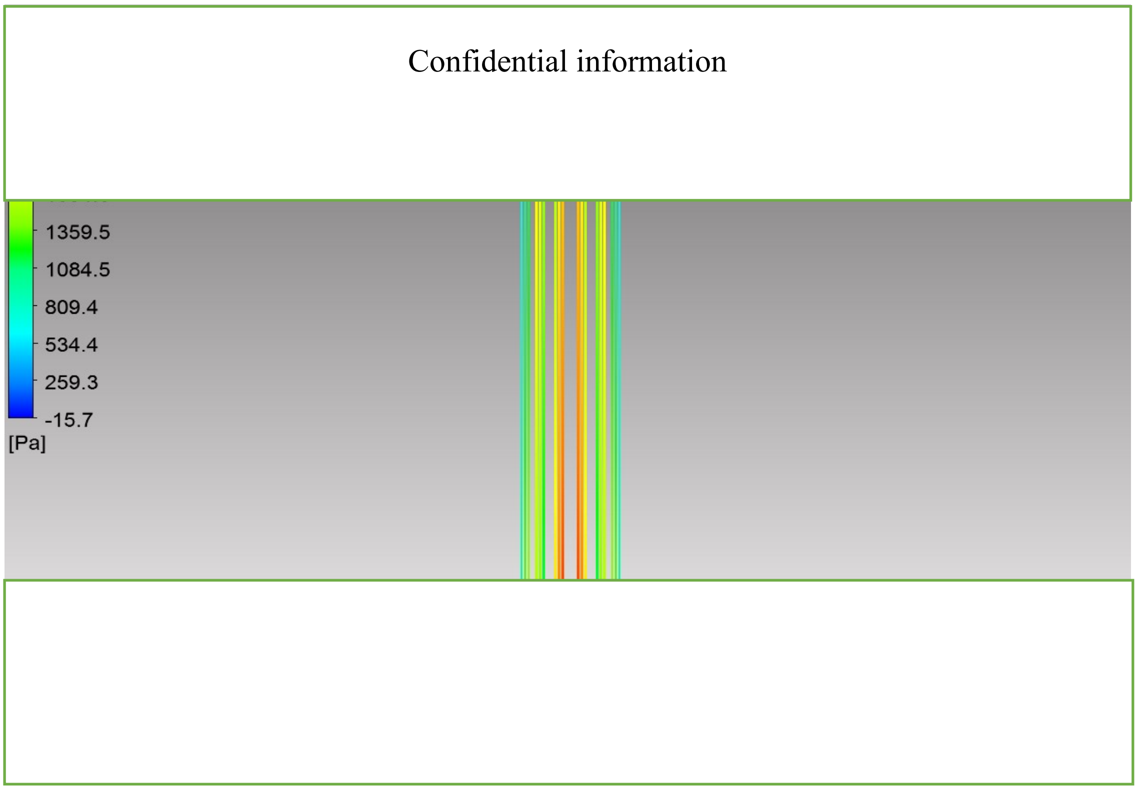

Figure 46 Milled

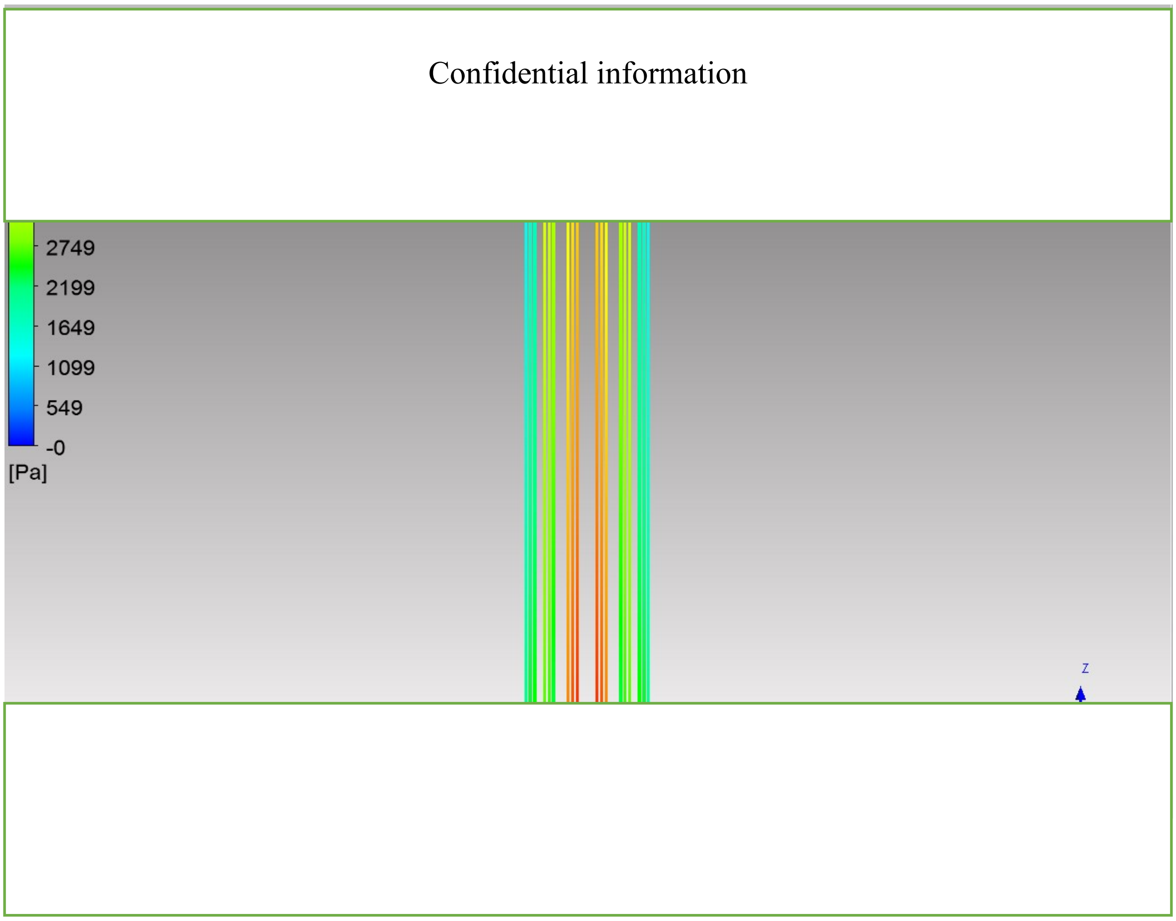

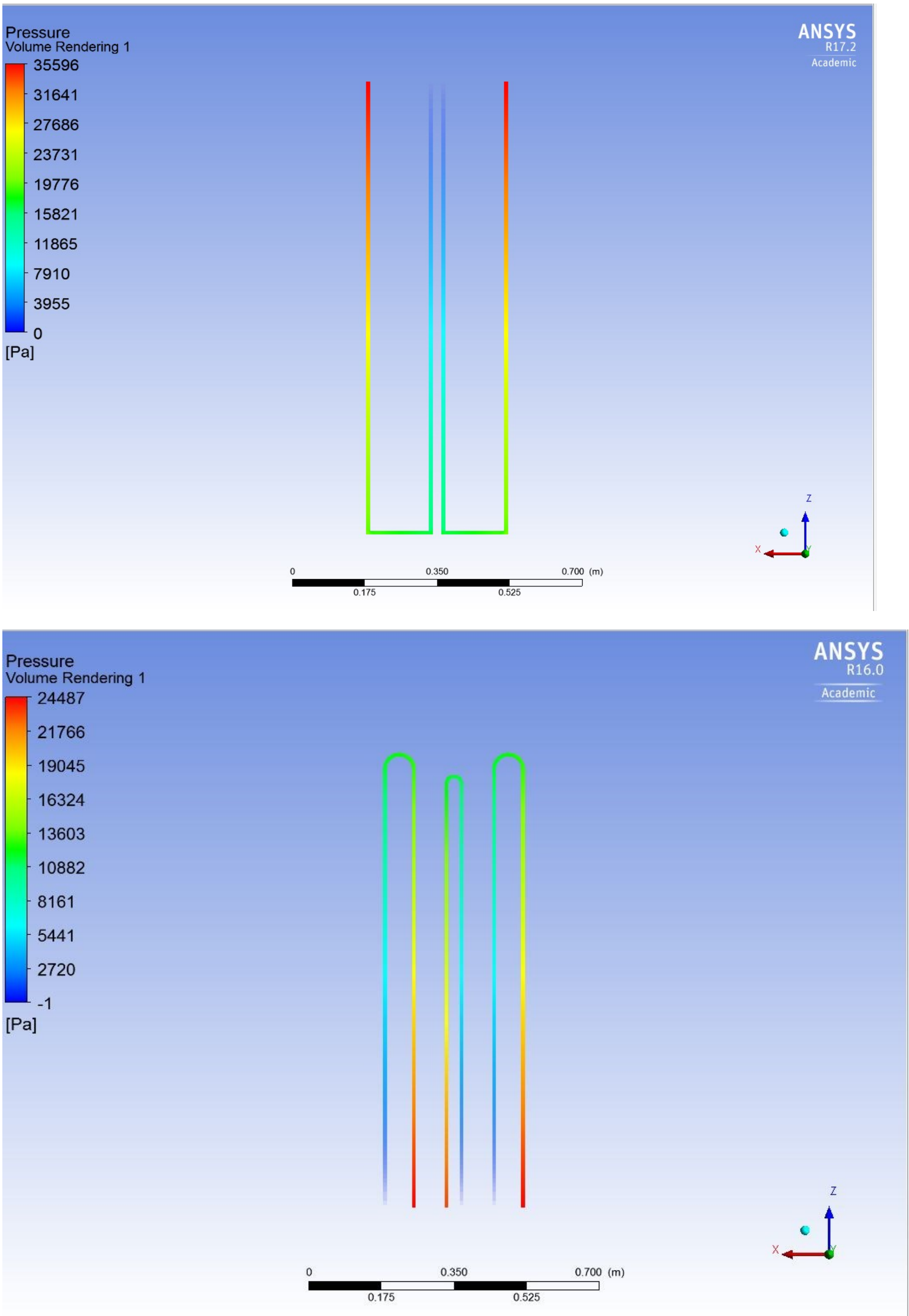

Figure 48 HFSC model 9 and 10

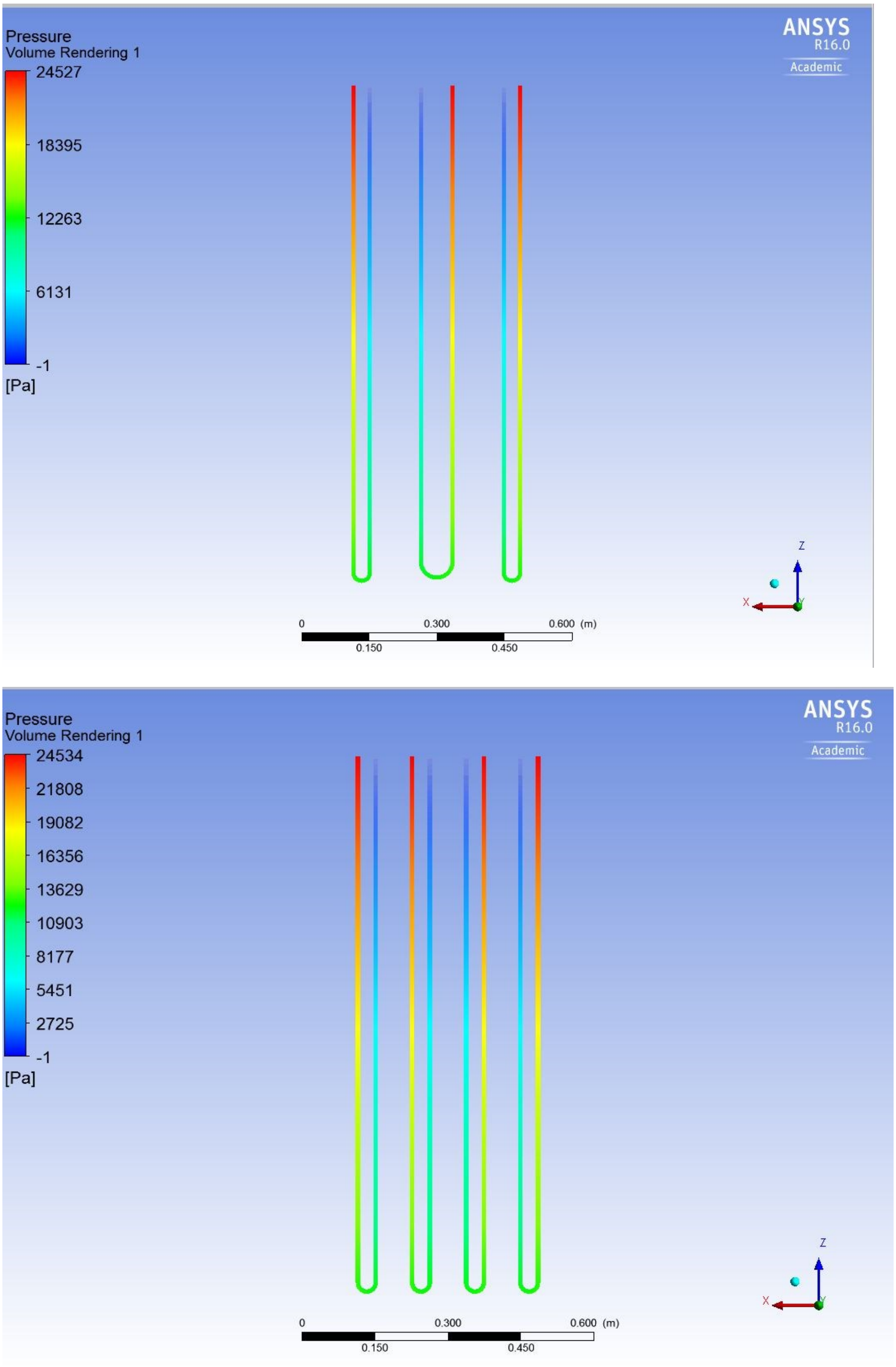

Figure 49 HFSC model 13 and 14

It can be seen from the pressure profiles that HFSC model 10, 13 and 14 maintains a higher pressure across the channel. Higher pressure is indicative of the roughness inside the channel.

Thus, after looking at all the simulation images and graphs above, **HFSC model 14** was chosen for further analysis.

8 Cost and Weight Analysis

Now that the differences in the thermal properties of the BCPs are seen, it remains to be seen if there is any benefit for the HFSC BCPs weight-wise and cost-wise. The following table shows the Weight of the separate components, the total weight and the total price of Materials. Since HFSC model 14 was chosen, analysis will only be done on it vs the Milled channel.

Table 3 Weight analysis

Model/Category	Volume of aluminum (m3)	Volume of Copper(m3)	Weight of Aluminum (kg)	Weight of Copper (kg)	Total weight (kg)	Total cost (euro)
Milled	0.00546993	0	14.77	0	14.77	77
HFSC model 14	0.0026868	0.00086	7.25436	7.7056	14.8	97

Now, for HFSC model 14 with copper plate at 1 mm thickness, the price of each product was found out to be 20 euros higher. But still HFSC model has far better cooling power than its Milled counterpart while having the same weight but lesser volume. Moreover, the number of processes it takes to produce a Milled channeled BCP is much higher than HFSC where only 1 operation can produce both the Channel and the welding.

Nevertheless, a further analysis was done to see if 0.8 mm thickness copper can have similar or close characterics. The result was can be seen below

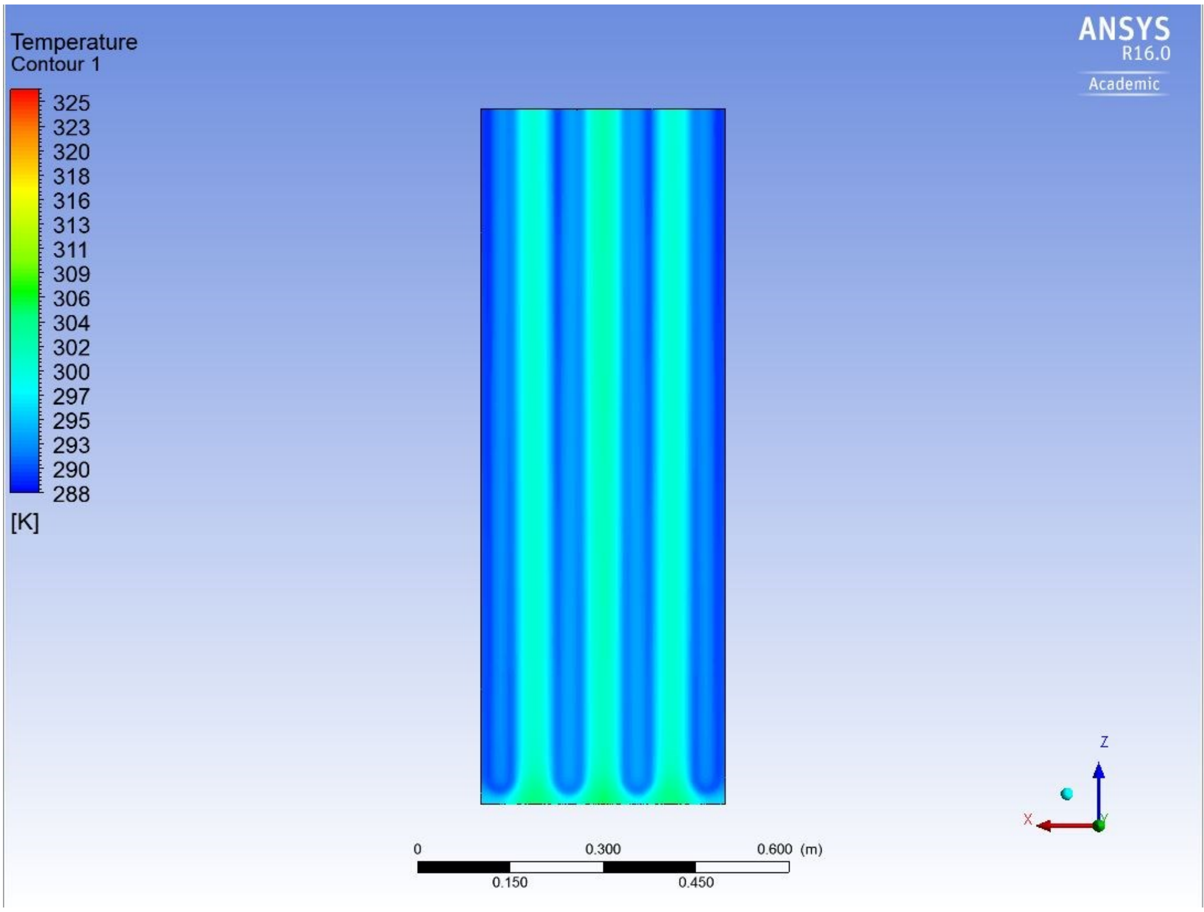

Figure 50 HFSC model 14 v2

The resulting simulation showed that the maximum temperature of the copper plate was just 2 Kelvin higher than its 1mm thick counterpart. Rest of the characteristics of HFSC model 14 v2 is almost same. So, cost analysis was done on this model again to see if there is any benefit.

Table 4 Cost and weight

Model/Category	Volume of aluminum (m3)	Volume of Copper(m3)	Weight of Aluminum (kg)	Weight of Copper (kg)	Total weight (kg)	Total cost (euro)
HFSC model 14 v2	0.0026868	0.0007	7.25436	6.272	13.4	86

Since there is a difference in the length of the channel, another important criteria for the BCP is its weight with water in it. The following observations were made when HFSC model 14v2 was compared to the milled and FSC BCP.

Table 5 Weight of water in the BCP

Model/Category	Volume of water(m^3)	Weight of water (kg)	Weight of system with water	Channel length
HFSC model14v2	0.000638	0.6368	14.0368	17.72m
Milled/FSC	0.0010864	1.084	15.854	39m

When comparing these two results, it can be seen that when the system has water flowing through it, the HFSC model has 11.5% lower weight than FSC or milled channeled BCP. Also, the channel length in HFSC model is 55% shorter than FSC or Milled BCP- This saves money as the channeling time gets reduced by over 50%.

Although the material cost for the HFSC models is more than the counterparts, the number of actual operations to achieve the final product is far less. This saves Machine and manpower cost. Moreover, the HFSC model 14 v2 has lower weight which was one of the goals of this thesis. Thus, HFSC model 14 v2 can be seen to be the best performing among all the options seen throughout this thesis.

9 Conclusion and future work

The following conclusions were drawn from the thesis:

Although not as reliable as the real experiments, CFD methods helps in testing out a concept or an idea without having to waste a lot of money and manpower. In this field of thermal management, the CFD is a strategic tool in support of testing and production. In this work, 14 HFSC models of different cooling paths for the BCP were simulated. Considering the hotspots values and distribution, from these initial models, 4 were selected for further evaluation.

The FSC model which was similar in every aspect to the milled model, except for the roughness. After the simulation, the peak of the FSC plate was found to be 4 Kelvin lower than that of the milled BCP. Since roughness was the only change, it can be inferred that roughness of the channel brought out this change in the temperature.

Copper's high thermal capabilities in form of high conductivity, high thermal effusivity and diffusivity helps in removing more heat from the batteries than the FSC and milled counterparts.

The variation of temperature across the HFSC plates were very low for most of the models. Regions with hot spots was seen, but even in those cases, the rest of the plate was at almost the same temperature. This could be attributed to the fact that copper can distribute heat across its surface in a much easier way than aluminum.

The simulation showed that the optimized model had 7% lower peak temperature than the milled model. The weight of the BCP by HFSC without water was lower than the BCP with the milled channel without water by 10%. With water flowing inside the BCP the difference in weight was 11.5%.

In addition to this, the HFSC model had 55% less channel length than the Milled channel. This means that the channeling operations on the HFSC channels are lesser and can save manhour and production cost.

9.1 Future work

With the flexibility while modelling HFSC plates, a lot can be achieved in this field in the future. But firstly, the interface gap between the copper and aluminum needs to be validated using experimental procedure. The two plates seems to touch each other when structural load is applied to the surface, but still, experimental validation could go a long way.

Additionally, HFSC allows for overlapping components to be welded together while producing a channel underneath. Using that idea, the concept of making copper fins on the surface of aluminum, or between the butted joint of two aluminum alloys could be explored. Since the sides of the batteries has the majority of the surface area, it could be good to try and make use of HFSC to make a way to take heat out of those large surfaces.

10 References

1. Thomas WM, Nicholas ED, Needham JC, Murch MG, Temple-Smith P, Dawes CJ. Friction welding. 1995 oct # ~24.

2. R.S. Mishra, Z.Y. Ma. "Friction stir welding and processing", Materials Science and Engineering R, 50, (2005), pp. 1-78. . 2005.

3. Mishra RS. Integral channels in metal components and fabrication thereof. 2005 aug # ~2.

4. Balasubramanian N, Mishra RS, Krishnamurthy K. Friction stir channeling: Characterization of the channels. Journal of Materials Processing Technology. 2009 21 April 2009;209(8):3696-704.

5. Nordal D, Karvinen H, Insinööritieteiden korkeakoulu, Vilaça P, Aalto-yliopisto, Aalto University. Design, development and analysis of tools for hybrid friction stir channeling [dissertation].

6. **Electric Drive** [Internet]. []. Available from: https://www.atec.ncsu.edu/innovation/electric-drive/.

7. Current Available EVs and their range [Internet]. []. Available from: https://evtide.com/evs.

8. J.-M. Tarascon MA. Issues and challenges facing rechargeable lithium batteries.

9. Young K, Wang C, Wang LY, Strunz K. Electric Vehicle Battery Technologies.

10. Jinlei Sun, Peng Yang , Rengui Lu, Guo Wei, and Chunbo Zhu. LiFePO4 Optimal Operation Temperature Range Analysis for EV/HEV.

11. **Tesla or GM: Who Has The Best Battery Thermal Management?** [Internet]. []. Available from: https://insideevs.com/tesla-or-gm-who-has-the-best-battery-thermal-management-bower/.

12. **BMW and LG Chem Trump Tesla in Battery Thermal Management** [Internet]. []. Available from: http://www.hybridcars.com/bmw-and-lg-chem-trump-tesla-in-battery-thermal-management/.

13. Versteeg HK, Malalasekera W. An Introduction to Computational Fluid Dynamics. Pearson; 1995.

14. ANSYS Inc. ANSYS FLUENT 12.0 User's Guide. . 2009.

15. SHARCNET. Fluent Documentation 16.2.

16. Adams T, Grant C. A Simple Algorithm to Relate Measured Surface Roughness to Equivalent Sand-grain Roughness. . 2012;1(1).

17. Heikki Karvinen, Afshin Hasani, Pauli Salminen, Tatiana Minav, Pedro Vilaça. Investigation of material properties and thermal efficiency of friction stir channeling applied to aluminum alloy AA5083. In press .

11 Appendix

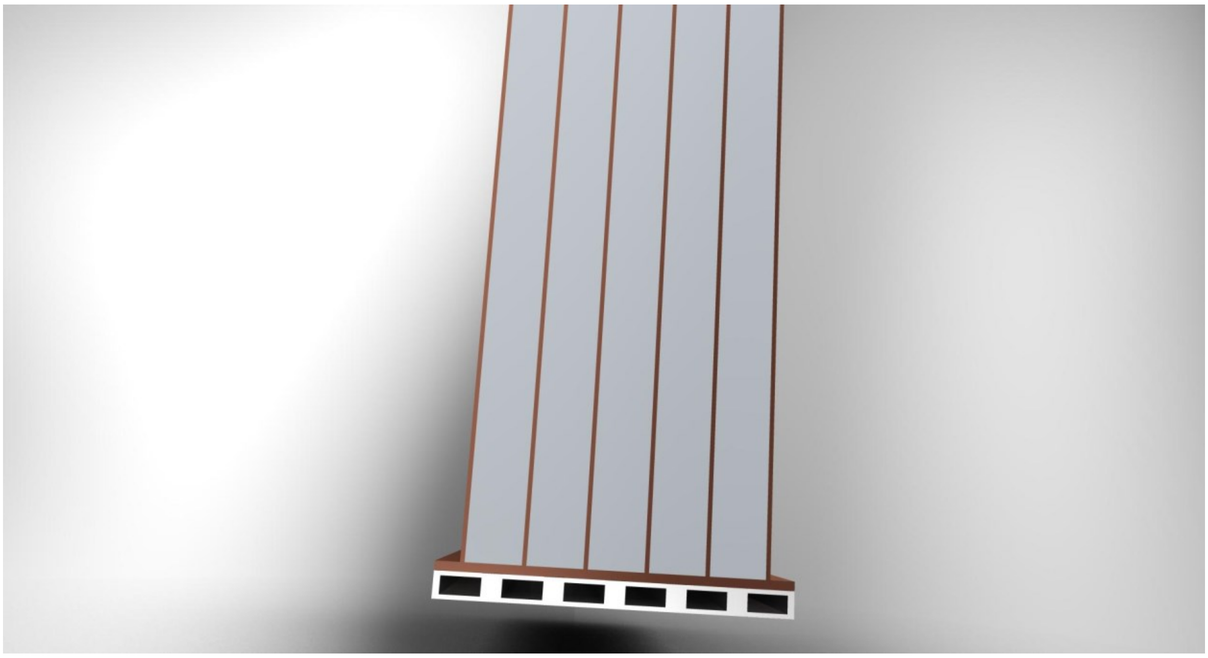

Figure 51 Example of Copper fin arrangement

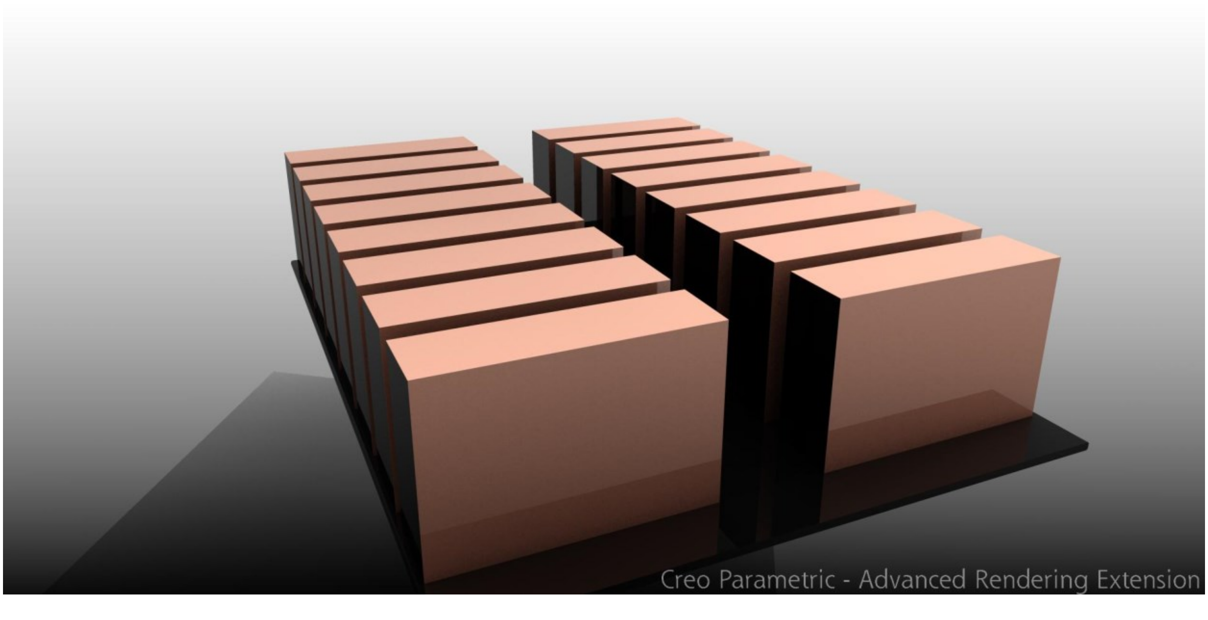

Figure 52 How the fins could be arranged